University College of Southeast Norway
Faculty of Technology

Master's Thesis
Study programme: Process Technology
Spring 2016

Abbas Ashimiyu Lawal

Measurement and correlation of data used for CO_2 absorption in different amine solutions at various temperatures

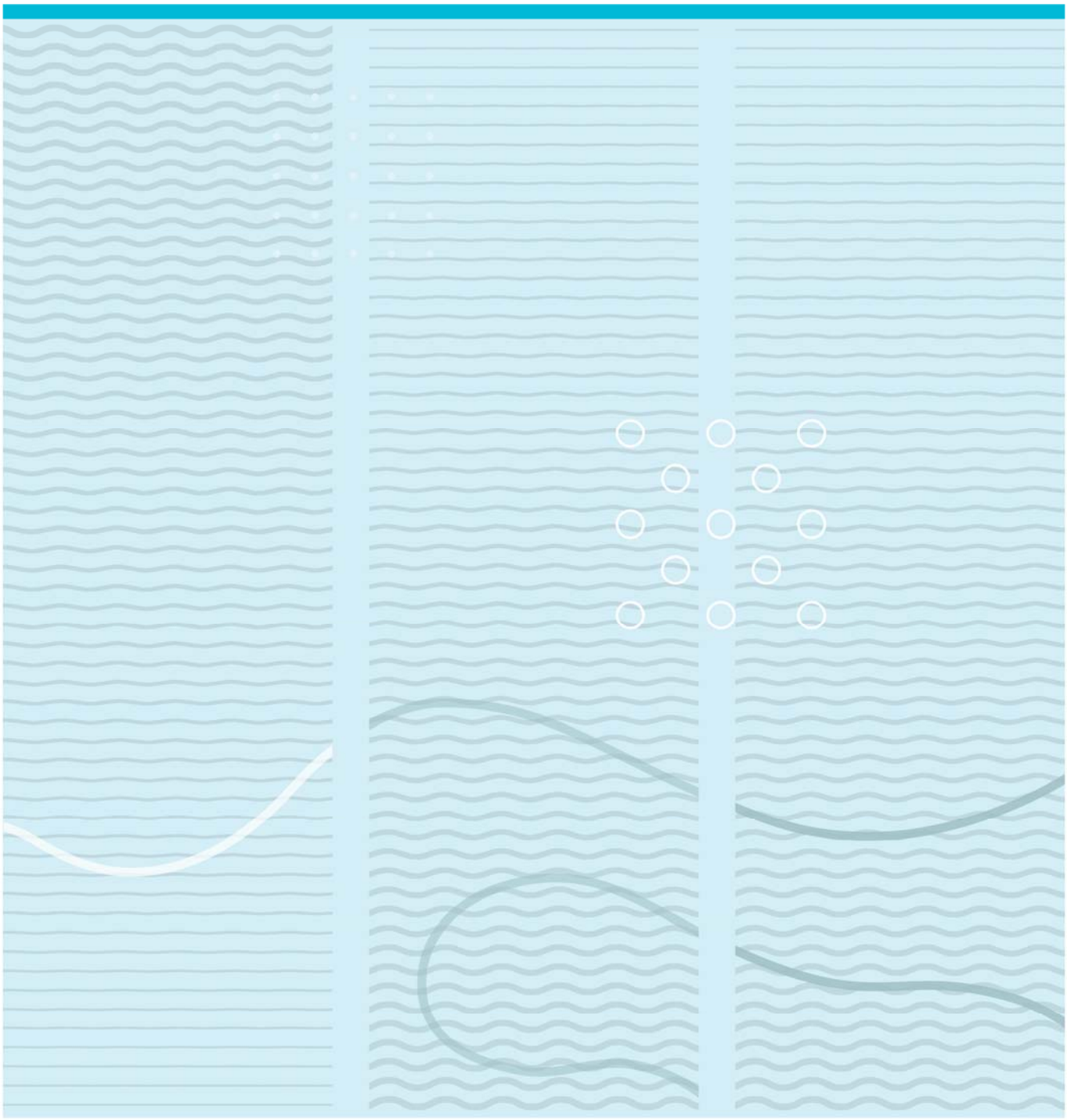

University College of Southeast Norway
Faculty of Technology

http://www.usn.no

This thesis is worth 30 ECTS

University College of Southeast Norway

MASTER'S THESIS, COURSE CODE FMH606

Student:	**Abbas Ashimiyu Lawal**
Thesis title:	**Measurement and correlation of data used for CO_2 absorption in different amine solutions at various temperatures**
Signature:	. . . . .
Number of pages:	< 80 >
Keywords:	. . . . .
	. . . . .
	. . . . .

Supervisor:	Professor Dag A Eimer	Sign.:	. . . . .
2nd supervisor:	Dr. Zulkifli Idris	Sign.:	. . . . .
Censor:		Sign.:	. . . . .
External partner:	Tel-Tek	Sign.:	. . . . .
Availability:	Open		

Archive approval (supervisor signature)**:** Sign.: . . . . . **Date :** . . . . . .

Abstract:

In order to design CO_2 absorption-desorption columns, models of experimental data would be needed to calculate many properties of the chemical system. In this research work, the experimental density values of aqueous solution containing monoethanolamine (MEA) and 3-dimethylamino-1-propanol (3DMA1P) as well as its constituent, MEA + 3DMA1P binary mixtures have been reported with their uncertainties in the temperature range, (298.15 to 353.15) K and atmospheric pressure, for 0.3 and 0.5 total amine mass fractions for the aqueous ternary system and whole composition range for the binary mixtures.

Excess molar volumes based on the density values were determined and correlated against mole fractions using Redlich-Kister model of the fourth order for the MEA + 3DMA1P binary mixtures and Nagata-Tamura model for the MEA + 3DMA1P + H_2O ternary solutions. The measured data and correlated data were compared and analyzed.

It is also reported in this work, the densities of aqueous solutions containing both *N*-methyldiethanolamine (MDEA) and piperazine (PZ) in a temperature range of (293.15 to 363.15) K. The mass fraction of PZ was varied in the range of 0 to 0.1 whilst keeping the mass fraction of MDEA constant at 0.3, 0.4 and 0.5. A non-dimensional single polynomial model was employed to correlate all the density values as a function of total amine mass fractions and temperature. The density values based on the model had a root mean square deviation of 0.0093kg/m^3 from the experimental values, which indicates an excellent agreement between the two values, considering a value of *0.414kg/m*^{3} for the combined experimental uncertainty, at 95% level of confidence.

Contents

Preface 6

1 Introduction 7

1.1 Objectives 7
1.2 Overview of thesis 8
1.3 Importance of study 8
1.3.1 Thermodynamic equilibrium models 8
1.3.2 Density 8
1.3.3 Excess molar volumes 8
1.4 System studied 9

2 Literature review 11

2.1 Amines 11
2.1.1 Reaction of CO_2 with Amines 11
2.2 Correlation and prediction methods 12
2.2.1 Classification of correlation and prediction methods 12
2.2.2 Previous work from literature 13

3 Experimental section 15

3.1 Materials and Apparatus 15
3.2 Experimental procedure 18
3.2.1 Preparation of samples 18
3.2.2 Density measurements 18
3.3 Errors and experimental uncertainties 21
3.3.1 Experimental errors 21
3.3.2 Assessment of experimental uncertainties 22

4 Results, correlations and discussion 26

4.1 MEA+3DMA1P+H_2O and MEA+3DMA1P systems 26
4.1.1 Densities 26
4.1.2 Excess molar volumes 37
4.2 Ternary system (MDEA + PZ + H_2O) 45

5 Conclusion 49

6 Further work 50

References 51

Appendices 55

Preface

This report presents the research work of my thesis carried out during Spring 2016 at University College of Southeast Norway, Telmark. The experimental work was carried out in CO_2 lab in collaboration with Tel-Tec research institute.

My profound gratitude goes to my supervisor, Professor Dag Eimer and co-supervisor Dr. Zulkifli Idris for their assistance and suggestions to support this research work.

Finally, I would like to express my gratitude to University of Southeast Norway for providing the opportunity to carry out this work.

1 Introduction

The scientific discovery of climate change is dated back to the early 19th century. During the 1960s, the threat of carbon dioxide emissions to the climate was made known by the scientists. This is very significant, as the climate change is a function of how the weather will be distributed in many years to come across the region of the globe [1].

The campaign of environmental protection against global warming caused mainly by CO_2 and other greenhouse gases has gained higher momentum in recent years, especially in many developed countries. The removal of CO_2 from large point sources - through carbon capture and storage (CCS) - is an important and necessary contribution to the success of this campaign. The CO_2 is removed by separating it from the produced gas streams. This method has been proved efficient in many process industries such as natural gas processing, coal gasification, and petroleum refining industries [2].

To capture CO_2, solution of alkanolamines such as monoethanolamine (MEA), diethanolamine (DEA), *N*-methyldiethanolamine (MDEA), piperazine (PZ) activated MDEA among others, has been frequently used industrially to absorb the CO_2 out of the natural, refinery, or synthetic gas streams [2]. An important reason why these amine-based solvents are being used is their selective affinity when reacting with CO_2, and this has made it a very useful technological process employed when capturing CO_2 from gas streams [3]. The excellent suitability of gas treating process using PZ activated MDEA solution lies in the high gas absorption rate and low energy requirement for regeneration in the gas processing unit, owing to high reaction rate of PZ with CO_2 and low reaction enthalpy of MDEA with CO_2 [4, 5].

1.1 Objectives

The study reported in this thesis is a necessary part of a big research project financed by the Norwegian Research Council which is aimed to predict equilibrium models for physicochemical data. The main objectives of this thesis are:

(1) To measure the density of selected binary, ternary systems of amine-based solutions at various temperatures, including estimation of experimental uncertainties.

(2) To correlate the density values and/or derived thermodynamic properties -such as the excess molar volumes- using selective predictive empirical models.

In this research, the solution densities of 16 binary systems, 22 ternary systems and 2 pure amine components were studied. The task description is available as Appendix A

1.2 Overview of thesis

This thesis report is segmented into 6 chapters. Chapter 1 is introduction. In chapter 2, a literature review is presented which gives a brief discussion of amines and their classes. It also gives an insight to the thermodynamic models for multicomponent solution. Chapter 3 is experimental section which explains the experimental procedure, material properties and assessment of experimental error and uncertainties. The results and correlations are shown and discussed in Chapter 4. Conclusion and further work are respectively presented in Chapter 5 and 6. Appendix is attached.

1.3 Importance of study

It is important to measure the densities of aqueous solution, and calculate the excess molar volumes from these experimental data and analyzing them, using empirical models. The reasons why this is important are discussed in sub-chapter 1.3.1, 1.3.2 and 1.3.3.

1.3.1 Thermodynamic equilibrium models

Laboratory data that are necessary for process optimization, design of columns, chemical reactors and other separation equipment should have an excellent and reliable representation of experimental data which are usually extensive. Researchers have resorted to be using flexible empirical models to represent these data so that it covers all important cases, and also protect the experimental results from being damaged [6].

1.3.2 Density

Density is generally a very significant physicochemical property of pure compounds and their solutions. This includes the amine-based solution, particularly in absorption-desorption processes [7]. Accurate values are needed in process control and optimization, mass transfer rate modelling and also for performing variety of related engineering calculations such as the Bayer process system for the recovery of gibbsite, $Al(OH)_3$ [8, 9].

1.3.3 Excess molar volumes

The excess molar volume is one of the excess thermodynamic properties of a solution which shows the difference between the actual property value and the ideal value of that solution at the same composition, temperature and pressure [10, pp. 413].

The excess molar properties are usually derived and calculated from physicochemical properties, such as densities and viscosities [7]. It is important to analyze the excess molar volumes because the values are used to understand the real behavior of the solution through the intermolecular forces and interaction in the mixture. The excess molar volumes can also be used to check and improve thermodynamic equilibrium models [11], as it will be illustrated in Chapter 4.

1.4 System studied

A wide variety of aqueous solution of single amines has been studied and used for CO_2 capture process for a number of years [12]. However, there has been a recent attention toward the thermodynamic study of mixed amines (a primary or secondary amine mixed with a tertiary amine) because of the high capture cost required for single amines which is in the range of 40-70 US$/ton of CO_2 [13]. This cost could be greatly reduced by combining the advantages of each individual amines to form mixed amines that require lower energy for regeneration in the absorption-desorption process [13].

The amine systems studied in this research work were carefully selected based on the fact that -to my best knowledge and that of my supervisors- no information available in the literature concerning the densities of methanolamine (MEA) + 3 –dimethylamino-1-propanol (3DMA1P) and aqueous solution containing MEA + 3DMA1P systems. In addition, the study was extended to the aqueous solution containing *N*-methyldiethanolamine (MDEA) + piperazine (PZ) due to insufficient information on the densities of the systems. Figure 1.1 shows the molecular structures of the amines considered in this work.

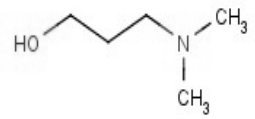

3-Dimethylamino-1-propanol (3DMA1P): [$C_5H_{13}NO$]

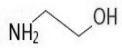

Monoethanolamine (MEA): [C_2H_7NO]

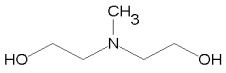

N-Methyldiethanolamine (MDEA): [$C_5H_{13}NO_2$]

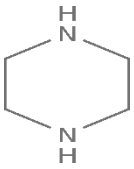

Piperazine (PZ): [$C_4H_{10}N_2$]

Figure 1.1: Molecular structures of the studied amines.

2 Literature review

This chapter covers a brief review of amines and their chemical reactions with CO_2 and also gives an insight to thermodynamic models for correlation and prediction of multicomponent solutions.

2.1 Amines

The derivatives of ammonia are organic compounds which contain nitrogen (N) atom at the same level of oxidation as ammonia. These derivatives are called *amines* when one, two or three of the hydrogen atoms has been replaced by organic groups containing carbon. When one carbon group is attached to N, they are known as primary amines (RNH_2), and secondary amines (R_2NH) when two carbon groups are attached. The tertiary amines (R_3N) are the ones with three carbon groups. An example of these types of amines are respectively methylamine, methylethanolamine and triphenylamine [14, pp. 1-3].

Sterically-hindered amines are another new class of amines recently introduced. The amine functional group in these amines possesses steric effect which makes them to look more commercially attractive over the conventional amines. An example of such amines is 2-amino-2-methyl-1-propanol (AMP) [15].

2.1.1 Reaction of CO_2 with Amines

There are two main reactions in CO_2 absorption with amines. The first reaction is known as *formation of carbamate* and the second reaction is the *hydrolysis of carbamate.* A balanced chemical reaction of both reactions are depicted in reaction (R2-1) and reaction (R2-2) respectively [16].

$$2RNH_2 + CO_2 \leftrightharpoons RNHCOO^- + RNH_3^+ \qquad \text{(R2-1)}$$

$$RNHCOO^- + H_2O \leftrightharpoons RNH_2 + HCO_3^- \qquad \text{(R2-2)}$$

where RNH_2, $RNHCOO^-$, RNH_3^+, and HCO_3^- represent alkanolamine, carbamate ion, alkanolamine with one proton, and bicarbonate ion respectively.

The *formation of carbamate* is the main body of reaction for primary and secondary amines because of the unrestricted rotation of the alkyl group around the amino-carbamate group due to stable carbamate compound. As a result, *hydrolysis of carbamate* hardly occurs for these classes of amines and thus, reaction (R2-1) shows the total reaction where 2 mol of alkanolamine is required to react with 1 mol of CO_2 [16].

There is lower stability of carbamate compound in sterically-hindered amines due to the restriction of the alkyl group to rotate around the amino-carbamate group. In this way, the hydrolysis of carbamate will occur, having bicarbonate ions and free amines as product when reacted with water [16], as shown in reaction (R2-2). Due to this, only 1 mol of the sterically hindered amines is required to react with 1 mol of CO_2. This is illustrated in reaction (R2-3).

$$RNH_2 + CO_2 + H_2O \leftrightharpoons RNH_3^+ + HCO_3^- \quad \text{(R2-3)}$$

This concludes that there is more stoichiometric capacity of absorption and desorption in sterically hindered amines than the conventional amines [16].

2.2 Correlation and prediction methods

In thermodynamics and phase equilibria of fluid mixtures, correlation and prediction method is a vital tool in describing the behavior of a real mixture using the properties of its pure components and existing experimental data. These methods can be very efficient in saving cost and time of conducting experiments, being the fact that they are based on use of equilibrium models. However, they are limited to the availability of experimental data [17, pp. 134-135].

It is very important to choose the correct models of the experimental data, as the errors associated with wrong models could have a very great impact on the design and optimization of chemical processes [17, pp. 135].

2.2.1 Classification of correlation and prediction methods

Correlation and prediction methods are classified into three groups. They are empirical, theoretical and semi-theoretical correlation methods. In empirical model, the available experimental data are fitted to some arbitrary function. This method has no basis on physical theory and interpolation could be carried out between the experimental data. However, one should be careful not to extrapolate such models to other physical systems or different fluid mixtures because the models are not based on physical theory.

The correlation and prediction method using theoretical models is based on physical theory and as such its models are suitable for interpolation and extrapolation, as long as the assumptions made during their development are taken into consideration [18, pp. 93].

The goal of the semi-theoretical method of prediction and correlation is to source information as much as possible from the few available data. The development of these type of models is on the basis of rigorous principle, by making simplifying assumptions and approximations to

develop a function which parameters cannot be measured, and are replaced with regression coefficients. This type of method is known as the *molecular thermodynamics* [18, pp. 92-94].

2.2.2 Previous work from literature

There has been many research on measurement and correlation of solution amine densities for various amine systems, with loaded and unloaded CO_2, and utilizing these data to study their thermodynamic properties using the correlation and prediction methods. Some selected previous literature on this type of methods are reviewed and presented.

Zhang et al. [19] measured the density and viscosity of partially carbonated aqueous tertiary alkanolamine solutions at temperatures between (298.15 and 353.15) K with mass fraction of alkanolamine at the range of 0.15 to 0.45. The density and viscosity of the solutions were successfully represented, using correlations as a function of temperature, CO_2 loading and amine concentration. The correlations agreed well with the experimental data.

Subham and Bishnupada [5] presented the density and viscosity of aqueous solutions of N-methyldiethanolamine + piperazine and 2-Amino-2-methyl-1-propanol + piperazine from (288 to 333) K, keeping the total amine concentration at 30%. The correlations as a function of temperature and amine concentration of both properties were in good agreement with the experimental data.

The density, surface tension, and viscosity of ionic liquids (1-ethyl-3-methylimidazolium diethylphosphate and 1,3-dimethylimidazolium dimethylphosphate) and ternary mixtures with aqueous MDEA, over the whole range of concentrations at (293.15−343.15) K were measured by Ghani et al. [12]. It was concluded that the correlations for all the physicochemical properties studied were less than 8% absolute percentage error and hence, the correlations were in good relation with the experimental data.

Han et al. [20] measured the density of water + diethanolamine + CO_2 and water + N-methyldiethanolamine + CO_2 from (298.15 to 423.15) K. The amine mass fraction range was at 0.3 to 1.0. The calculated excess molar volumes and densities were correlated using Redlich-Kister model [6] and Weiland model [9] respectively, and the deviations between the measured data and correlated data were less than the experimental error.

In another journal paper, Han et al. [21] also measured the density of water + monoethanolamine + CO_2 from (298.15 to 413.15) K and surface tension of water + monoethanolamine from (303.15 to 333.15) K. The Redlich-Kister [6] model was also used to correlate the excess molar volumes. The models fitted to the data were satisfactory.

Recently, Wang et al. [22] measured the densities of the binary system (N-methyldiethanolamine + (2- aminoethyl) ethanolamine) and its ternary aqueous mixtures from 283.15 to 363.15 K. The calculated excess molar volumes of the ternary system was predicted using six different models. They are Redlich-Kister, Kohler, Jacob-Fitzner, Tsao-Smith, Toop, and Scatchard models. The best agreement with the experimental data was achieved by Redlich-Kister, Kohler, and Jacob-Fitzner models. Higher deviations were seen for that of Tsao-Smith and Toop.

Zulkifli et al. [23] reported the densities of unloaded and CO_2 loaded 3-demethylamino-1-propanol solutions at temperatures of (293.15 to 343.15) K. Additionally, the values of excess molar volume of the unloaded systems were produced and correlated. Thermal expansion values were also reported. The model of [9] was used successfully to represent the densities of the CO_2 loaded solutions.

Densities and viscosities of both piperazine (PZ) and MDEA aqueous solutions were determined at different PZ and MDEA concentrations by Derks et al. [24]. The temperature range observed was (293.15 – 323.15) K. They also measured the liquid diffusivities of PZ solutions using the Taylor dispersion technique with temperature range of (293.15 – 368.15) K.

In a further development, Diky et al. [25] developed a first full scale software implementation algorithm, which was named a ThermoData engine (TDA). This developed software was able to evaluate thermo-physical properties of ternary chemical systems. It constructed Redlich-Kister type of equations for properties such as excess volume, viscosity, surface tension and thermal conductivity among others.

3 Experimental section

This chapter shows the materials and apparatus used in this research and an outlined experimental procedure that was carried out in the laboratory. It also covers the experimental errors and uncertainties in the experiment.

3.1 Materials and Apparatus

A total of four amine chemicals, and water were studied in this thesis. The amines are MEA, 3DMA1P, MDEA and piperazine. Methanol was used as a cleaning fluid. All the amines were sourced from Alfa Aesar and Sigma Aldrich Companies and their purities were kept as supplied, without additional purification. Although, they were degassed. Table 3.1 shows the description of the chemical samples including their molecular weight (kg/kmol).

Table 3.1: Chemical sample descriptions[a]

			Molecular weight
Chemical name	**Source**	**Purity**	**kg/kmol**
Monoethanolamine (MEA)	Alfa Aesar	$x \geq 0.99$	61.08
3-Diethylamino-1-propanol (3DMA1P)	Alfa Aesar	$x \geq 0.99$	103.16
N-methyldiethanolamine (MDEA)	Sigma Aldrich	$x \geq 0.99$	119.16
Piperazine (reagent grade)	Sigma Aldrich	$x \geq 0.99$	86.14
Water (H_2O)		18.2 MΩ cm	18.015
Ethanol			

[a]Purities are as reported by the manufacturer, the value shown for water is resistivity. Molecular weights are calculated from the chemical formulas. Ethanol was used for cleaning the measuring cell.

The main apparatus used for this project is the Antor Paar DMA 4500 density meter. Other apparatus used are the rotary pump, precision balance scale, magnetic stirrer with stir bars, flasks, syringes and pipettes.

The DMA 4500 of the Anton Paar density meter is based on oscillatory U-tube method with two integrated platinum thermometers (Pt 100) controlling the temperature. It has a total of 10 methods of measurement in which any of the method could be selected, and the output results can be converted into specific gravity, concentration or other density related units by utilizing inbuilt functions as well as conversion tables. The result is displayed on the programmable LC screen. The density meter is limited to measure in the temperature range of (273.15-363.15) K and at normal atmospheric pressure. The complete structure of the density meter is depicted in Figure 3.1.

Figure 3.1: The density meter structure in operation.

The rotary evaporator set up is shown in Figure 3.2. The rotary evaporator was used to remove solvents that could be present in the pure liquid chemicals before preparing samples. The operating mode, procedure and detailed instruction manual is attached as Appendix B.

Figure 3.2: Rotary evaporator setup in operation mode.

The precision balance scale used in this work is the Mettler Toledo (XS-403S) type. Figure 3.3 shows the structure of the balance scale.

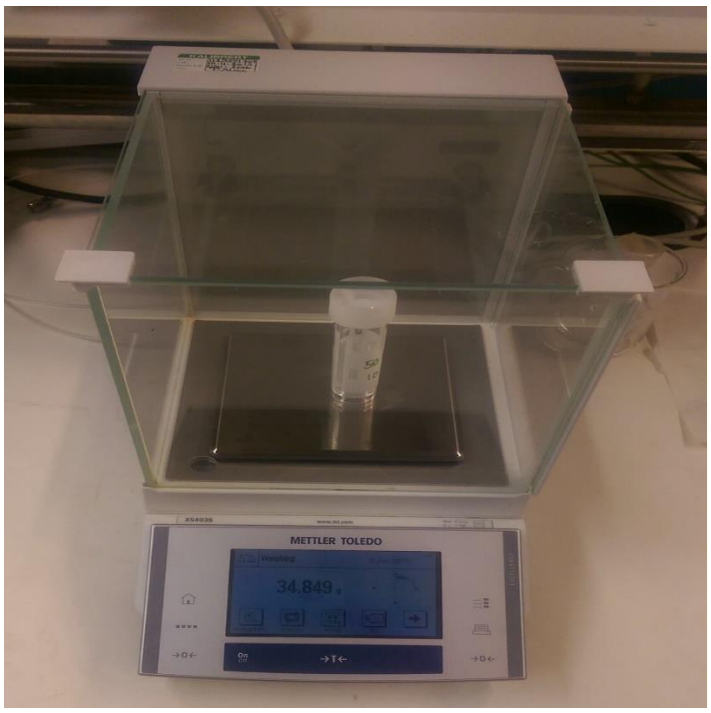

Figure 3.3: Mettler Toledo precision balance scale in operation.

The stirrer is a magnetic type. It works on the principle of magnetic field which set the stir bar into a rotational motion, thus stirring the mixture in the flask. It was mainly used to homogeneously mix the MDEA + PZ + H2O ternary systems due to the presence of the alkaline deliquescent crystals (PZ) in the solutions. Figure 3.4 shows the stirrer in use.

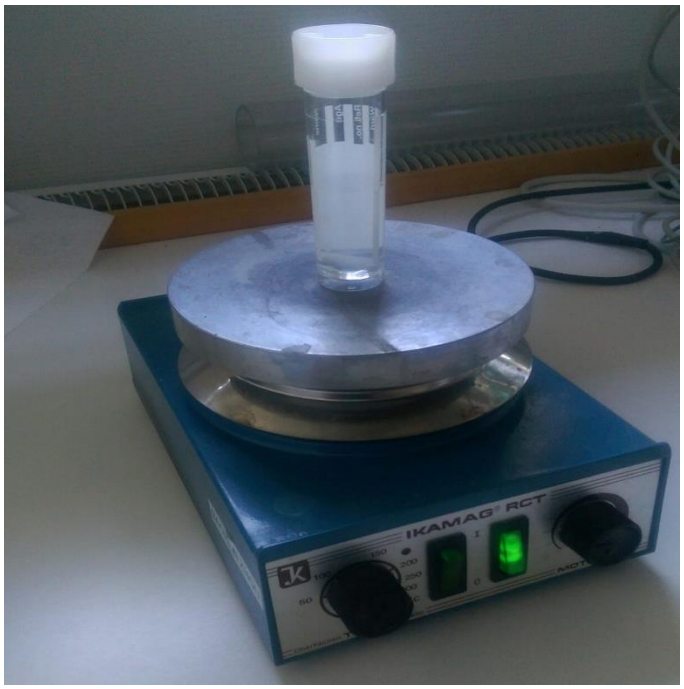

Figure 3.4: Magnetic stirrer with stir bar in operation.

3.2 Experimental procedure

3.2.1 Preparation of samples

All the required chemicals used in this work were weighed using the Mettler Toledo (XS-403S) analytical balance having an accuracy of $\pm 1 \times 10^{-6}$ kg. The liquid chemicals were all degassed by the rotary evaporator before mixing. The procedure for degassing the samples is available at Appendix B.

Aqueous ternary mixtures of MEA + 3DMA1P + H_2O were prepared by weighing and mixing the pure amine components with degassed Milli-Q water. The binary mixtures of MEA + 3DMA1P were prepared by mixing the required pure amine components. Aqueous ternary solutions of MDEA + PZ + H_2O were prepared by dissolving known amounts of PZ crystals in a required mass of degassed Milli-Q water and a known amount of MDEA was added to the mixtures. The mixtures were agitated to a total dilution using the magnetic stirrer.

It is to be noted that the amine mass concentration values used in this work are all based on the weighted mass of amine components and water in the mixtures. This is justified on the conclusion of Zulkifli et al. [23, 26] in their work that there is negligible difference of mass concentration between the acid-base titration values and weighted mass preparation values. It is important to state that the sample preparation procedure in this work is the same as that of the work of [23, 26].

3.2.2 Density measurements

The densities of pure water, pure MEA, pure 3DMA1P, MEA + 3DMA1P + H_2O, MDEA + PZ + H_2O ternary solutions, and MEA + 3DMA1P binary mixtures were measured using the Anton Paar (Austria) DMA 4500 density meter. Before measuring any of the samples, cleaning of the measuring cell was perfected using ethanol and degassed water. The water was used to remove sample leftover that may be present in the cell, while the ethanol was used to remove the water residue, and then evaporated using a stream of dry air and by turning on the air pump using the 'PUMP' key on the density meter. The measuring cell was left to dry for at least 10 minutes before turning off the air pump.

According to the instrument specification, the density meter was calibrated before density measurements. In calibrating the instrument, the density data of water at different temperatures, (298.15-353.15) K were measured and compared with the density data of Bettin and Spieweck [27]. The measured density values for this work and that of Bettin and Spieweck [27], with the

corresponding absolute deviations, calculated by equation (3-1) are listed in Table 3.2. The comparison between the two densities can be observed better in Figure 3.5.

Table 3.2: Comparison between the measured density values and literature values of pure water at varying temperatures and constant atmospheric pressure.

	Density (kg/m^3)		
Temperature (K)	**This work**	**Literature data**	**Absolute deviation (kg/m^3)**
298.15	997.07	997.04	0.03
303.15	995.67	995.65	0.02
308.15	994.05	994.02	0.03
313.15	992.24	992.21	0.03
318.15	990.24	990.21	0.03
323.15	988.06	988.03	0.03
328.15	985.72	985.69	0.03
333.15	983.23	983.19	0.04
338.15	980.59	980.55	0.04
343.15	977.81	977.76	0.05
348.15	974.89	974.83	0.06
353.15	971.84	971.79	0.05

$$AD(kg/m^3) = \left|\rho_{\exp,i} - \rho_{ref,i}\right| \qquad (3\text{-}1)$$

AD is the absolute deviation; $\rho_{\exp,i}$ and $\rho_{ref,i}$ in kg/m^3 are respectively this work densities and reference densities.

The combined expanded uncertainty $U_c(\rho)$ of the density measurements is 0.147 kg/m^3 (*95%* confidence level, *k=2*, *Norm*), taking into consideration the instrumental (0.05 kg/m^3) and temperature change (0.023 kg/m^3) standard uncertainties. A detail procedure of how the uncertainty values are calculated is shown in sub-chapter 3.3.2.

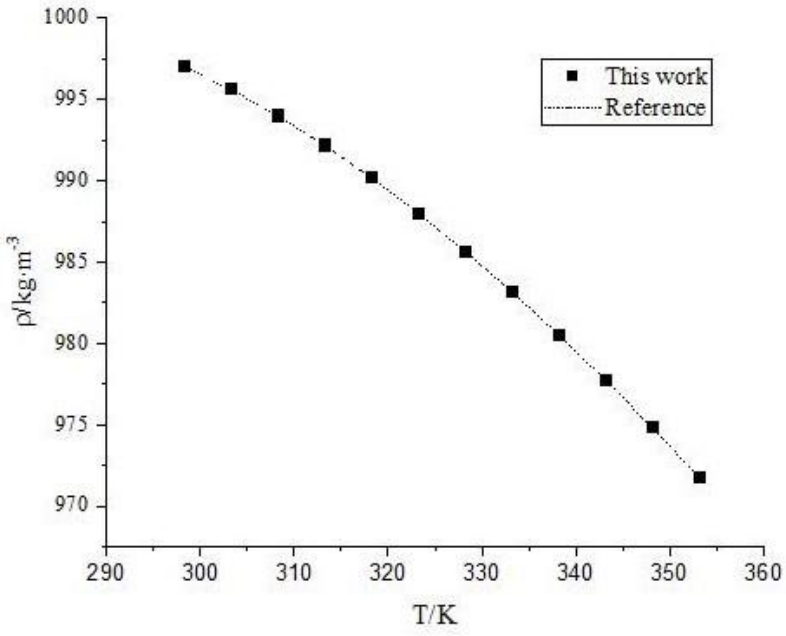

Figure 3.5: Density of water measured in this work (symbol) and that of Bettin and Spieweck [27] (dotted lines) at various temperatures and constant atmospheric pressure.

It can be observed from Figure 3.5 and Table 3.2 that the densities of water from this work are in good agreement with the reference data, at an average absolute deviation, AAD (calculated by equation (3-2)) of 0.037 kg/m^3, which is within the experimental uncertainty (0.147 kg/m^3) and as such, it can be concluded that the density meter is functioning properly.

$$AAD(kg/m^3) = \frac{\sum_{i=1}^{N} \left| \rho_{\exp,i} - \rho_{ref,i} \right|}{N} \qquad (3\text{-}2)$$

AAD is the average absolute deviation; $\rho_{\exp,i}$ and $\rho_{ref,i}$ in kg/m^3 are respectively this work densities and reference densities. *N* is the number of experimental points.

As a quality control procedure, density checks were performed with degassed water at 293.15K before measuring any of the samples. All the density measurements were performed ONLY after an OK message was received from the density meter. In the few cases where the density check was repeatedly not OK after re-cleaning the cell thoroughly, air and degassed water at 293.15 K were used to adjust the instrument. The details of the calibration, density check and adjustment procedures are attached as Appendix C.

To measure the densities, each sample free of bubbles was injected into the measuring cell by a 10 *ml* syringe and was left at the filling inlet to prevent leakage, with part of the sample present in the syringe. The instrument was then set to the required temperature value (in degrees

Celsius) for the sample and the "START" soft key was pressed. The density value was displayed on the screen after the cell has reached equilibrium. When air bubble(s) were/was noticed, usually at high temperatures, the used sample in the cell was substituted by the unused sample left in the syringe before proceeding with measurement. It took an average estimate of 8 minutes for the temperature of the cell to increase by 5^{o}C before displaying the density value on the screen. It is important to mention that each set of experiments in this work was triplicated and the average values are the ones reported in this thesis report.

3.3 Errors and experimental uncertainties

3.3.1 Experimental errors

It is impossible to measure the true or exact value of any physical quantity. When there is a difference between a measured value and the corresponding true value, the result is known as "error". Error can be divided into systematic error and random error. A systematic error is one that arises as a result of the difference between the experimental arrangement and assumed theory in the absence of correction factor. It is often cause by wrong use of instruments or malfunction of the data handling system of the instruments. A random error on the other hand, is one that usually changes and always present throughout the set of measurements. It arises as a result of uncertain or unknown changes in the experiment. It can be detected and minimized by repeating the measurement in number of times and taking the average [28, pp. 5-8]. This explains why the density measurements in this work were measured three times, and the average values reported.

3.3.1.1 Bubble Propagated Error (BPE)

During the density measurements, I noticed that an important systematic error that the experimenter should be cautioned of is what I termed the "Bubble Propagated Error (BPE)". More often than not, bubbles can be encountered in the sample in the measuring cell during density measurements at high temperatures, depending on the physicochemical properties of the measured liquid. To demonstrate the effect of BPE on measured density values, the density of an MEA solution sample was measured differently at 338.15K, with and without bubbles. A true value of 989.92 kg/m^3 was recorded without bubbles and 983.97 kg/m^3 with two very small diameters air bubbles which were almost unnoticeable. The error is 1% of the true value. This is relatively large, considering the difference between any two density values at different temperatures as it can be observed in Table 4.2 and Table 4.4.

From my research experience in the lab, in order to have a BPE free density values, I recommend that presence of bubbles should be carefully checked in the sample in the measuring cell before recording any density value displayed on the density meter screen. If bubble(s) is/are found, the used sample in the cell should be carefully substituted by the remaining unused sample in the syringe. If presence of bubbles are repeatedly noticed after changing the samples, the temperature of the cell should be set back to 20^{o}C. When the cell is on average of 20^{o}C, a new sample should be injected and then the measuring cell is set to the required high temperature. This has worked for me a number of times. The best possible explanation for this procedure is that there is a little bit of disturbance in the sample in the cell when density values are taken at regular temperature intervals. It is well known that, when liquids are agitated or rough handled, they tend to form bubbles. This recommended procedure would reduce the disturbance on the sample, and as such, the tendency to form bubbles is minimized. If the BPE still persist, then, it can be concluded that the sample cannot be accurately measured at that high temperature using the DMA 4500 density meter, and as such, a high pressure U-tube (DMA HP) which can restrain evaporation must be used.

3.3.2 Assessment of experimental uncertainties

The range of values (plus or minus) where the output value of a measurement lies is known as *uncertainty*. It is a measure of how accurate a measurement could be. A high measurement accuracy indicates low uncertainties and a low measurement accuracy implies high uncertainties [29, pp. 1-2].

The correctness and precision of physiochemical data sourced from the laboratory has a great impact on process design and calculations. With proper knowledge of the uncertainties, a process engineer would be able to access the level of risk involved in using the data [30]. It is therefore important to assess the uncertainties involved in performing these experiments. The assessment of uncertainties in this experiment is based on the Guide of Measurement Uncertainty in Chemical Analysis [31].

The procedure to estimate the uncertainty of the experimental results in this report consists of four main steps. To make it easily readable, the uncertainty estimations are done simultaneously with the procedures.

1. Specifying the measurand.

The measurand is density, because it is what we are measuring, i.e. the final output.

2. Identifying all relevant sources of uncertainty for the measurand.

This procedure is usually one of the most important and difficult step in estimating uncertainties because of the risk of neglecting important sources of uncertainties which could undermine experimental results, because an important source has been left out. This risk could be minimized by using what is called "a cause and effect diagram" which its application is demonstrated as shown in Figure 3.6, showing the most important sources of uncertainty in this experimental work.

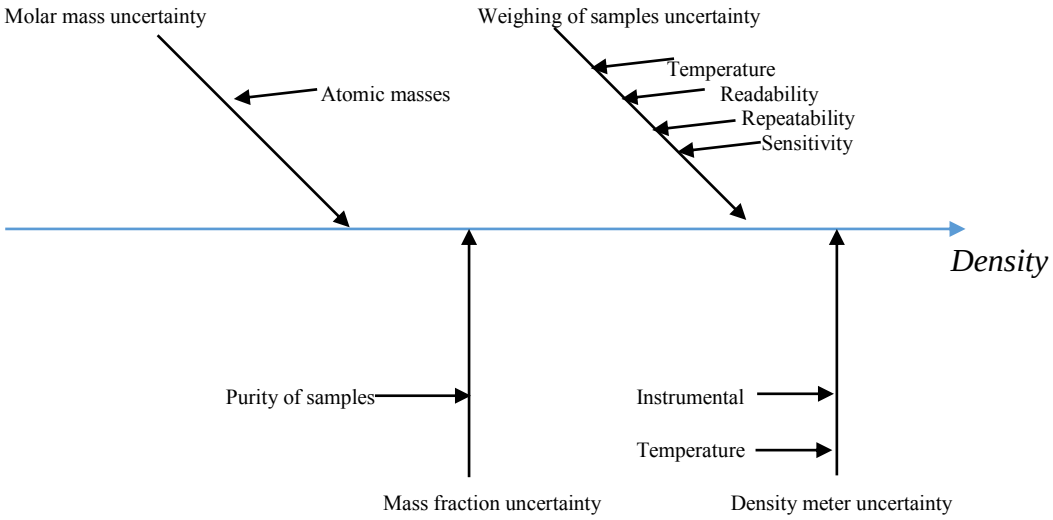

Figure 3.6: A cause and effect diagram of uncertainty sources in experimental determination of Density.

The uncertainty due to molecular mass -which is mainly from the combination of the uncertainty in the atomic masses of its constituent elements- of samples, and weighing of samples can be neglected. This is because the values would be very negligible ($\leq 10^{-6}$) when combined with the relatively high standard instrumental uncertainty ($0.05 kg/m^3$).

3. Quantifying the different sources of uncertainties.

The uncertainty of measured densities considered in this work is the combination of the uncertainties from the density meter and the mass factions. The uncertainty sources for the density meter are that resulting from temperature accuracy and instrument density accuracy (Figure 3.6). A value of ± 0.03 K and ± 0.05 kg/m^3 for temperature and the instrument respectively was reported from the manufacturer. In the case of the mass fractions, the uncertainties were estimated from the purity of the components (≥ 0.99) as shown in Table 3.1. The uncertainty for all the mass fractions is then 0.01.

Considering the densities of the binary (MEA + 3DMA1P) and the ternary (MEA + 3DMA1P + H_2O) system, the experimental uncertainty is a function of temperature, instrument density, and mass fractions (w_1 and w_2) of MEA and 3DMA1P. These uncertainties are quantified using the *sensitive coefficient* method [31], calculated by equation (3-3).

$$c_i = \frac{\delta f}{\delta x} \tag{3-3}$$

c_i is the sensitive coefficient, $\frac{\delta f}{\delta x}$ is the gradient of property *f* against input *x*.

The maximum gradient of density for the MEA + 3DMA1P binary systems was calculated to have an absolute value of $0.796 kg/(m^3 \cdot K)$ against temperature and $203.1 kg/m^3$ against mass fraction of MEA, which is equally the same for the mass fraction of 3DMA1P and thus, having a total sensitive coefficient value of $406.2 kg/m^3$ for the mass fractions.

The maximum gradient of density for the MEA + 3DMA1P + H_2O ternary systems has an absolute value of $0.496 kg/(m^3 \cdot K)$ against temperature and *107.2 kg/m*^{3} against mass fraction of MEA and $107.2 kg/m^3$ against mass fraction of 3DMA1P.

The uncertainty of the density of (MDEA + PZ + H_2O) solutions is a function of the temperature, instrument density, and mass fractions of MDEA and PZ. The calculated maximum gradient of density has an absolute value of $0.650 kg/(m^3 \cdot K)$ against temperature and $184.3 kg/m^3$ against mass fraction of MDEA and $56.1 kg/m^3$ against mass fraction of PZ.

4. Calculating measurement uncertainty

To finally calculate the combined standard uncertainties, the different uncertainty parameters estimated in step 3 would be utilized. The combined uncertainties together with the instrumental standard uncertainty from the manufacturer (0.05kg/m^3) are calculated by equation (3-4).

$$u_c = 0.05 kg/m^3 + \sqrt{c_1 u_1^2 + c_2 u_2^2 ..... c_n u_n^2} \tag{3-4}$$

u_c is the combined standard uncertainty; u_i is the reported uncertainty of parameter *i;* c_i is the sensitive coefficient of parameter *i.*

The calculated maximum combined expanded uncertainty for density measurements $U_c(\rho)$ calculated by equation (3-5) for: MEA + 3DMA1P binary systems is 0.501 *kg/m*^{3} (coverage factor *k* = 2, *Norm.)*, MEA + 3DMA1P + H_2O ternary systems is 2.082 *kg/m*^{3} (*k* = 2, *Norm.)*,

and for MDEA + PZ + H_2O ternary systems is 0.414 (k = 2, *Norm.)*, all at 95% level of confidence.

$$U_c(\rho) = k \cdot u_c \qquad (3\text{-}5)$$

$U_c(\rho)$ is the combined expanded uncertainty, k is the coverage factor and u_c is the combined standard uncertainty.

It is important to state that the uncertainties were calculated based on the assumptions that uncertainty sources are independent of one another and the uncertainty due to the purity of water is negligible.

4 Results, correlations and discussion

This chapter presents the measured density data, correlations and discussion. In order to ease understanding, the chapter is divided into two sections. The first section (Chapter 4.1) is the binary (MEA+3DMA1P) and the ternary (MEA+3DMA1P+H_2O) systems, while the second section (Chapter 4.2) is the MDEA + PZ +H_2O ternary systems.

4.1 MEA+3DMA1P+H_2O and MEA+3DMA1P systems

4.1.1 Densities

The densities of pure MEA, 3DMA1P were first measured and compared with known values in the literature [21, 23]. The densities are listed in Table 4.1, including the absolute deviations (AD) which were calculated using equation (3-1). The experimental uncertainties were calculated using the same procedure in Chapter 3.3.2. The combined expanded uncertainty $U_c(\rho)$ for the density measurements of pure MEA and 3DMA1P are respectively *0.153 kg/m^3* and *0.154 kg/m^3*.

Table 4.1: Comparison between the measured density values and literature values of pure MEA and 3DMA1P at varying temperatures and constant atmospheric pressure ($P = 0.1013 MPa$).[a]

		Density (kg/m^3)		
Component	**Temperature (K)**	**This work**	**Literature data [21]**	**AD (kg/m^3)**
MEA	298.15	1011.86	1011.9	0.04
	303.15	1007.9	1008	0.1
	308.15	1003.92	1004	0.08
	313.15	999.94	1000	0.06
	318.15	995.94	996	0.06
	323.15	991.92	992	0.08
	328.15	987.89	988	0.11
	333.15	983.84	983.9	0.06
	338.15	979.78	979.8	0.02
	343.15	975.69	975.8	0.11
	348.15	971.58	971.6	0.02
	353.15	967.45	967.5	0.05
			Literature data [23]	
3DMA1P	298.15	881.12	884	2.88
	303.15	877.12	879.8	2.68
	308.15	873.13	875.5	2.37
	313.15	869.11	871.2	2.09
	318.15	865.07	866.8	1.73

Table 4.1 (Continued)

		Density (kg/m^3)		
Component	**Temperature (K)**	**This work**	**Literature data**	**AD (kg/m^3)**
3DMA1P	323.15	861.01	862.4	1.39
	328.15	856.92	858	1.08
	333.15	852.81	853.5	0.69
	338.15	848.68	849	0.32
	343.15	844.5	844.4	0.1
	348.15	840.3	-	-
	353.15	836.07	-	-

[a]Standard uncertainties *u* are *u(T)=0.03 K*, *u(P) =2.0kPa*, instrument standard uncertainty = *0.05kg/m^3*. The combined expanded uncertainty for density measurement $U_c(\rho)$ for MEA and 3DMA1P are respectively *0.153kg/m^3* and *0.154kg/m^3*.

The overall maximum AD value is *2.88 kg/m^3* at *298.15K* for 3DMA1P. The average absolute deviations, calculated from equation (3-2) for MEA and 3DMA1P are (0.0658 and 1.5330) kg/m^3, respectively. The comparison can be observed better in Figure 4.1. It can be observed that the deviations are small and are within the acceptable experimental uncertainties

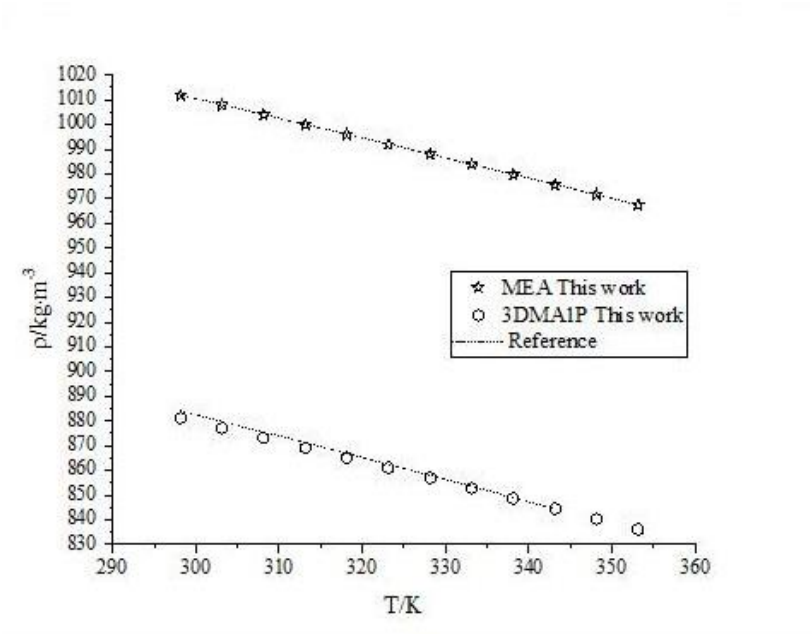

Figure 4.1: Density of pure MEA and 3DMA1P measured in this work (symbol) and that of [21] and [23] (dotted lines) at various temperatures and constant atmospheric pressure.

This concludes that the experimental apparatus used in this work are accurate and the density determination is reliable. However, the density values for 3DMA1P at (348.15 and 353.15) K could not be compared because they are not reported in any of the literature searched.

The densities of the binary system (MEA + 3DMA1P) were measured at different mass fractions in full range of 0.10 to 1.00, while the temperature was varied from (298.15 to 353.15) K at 5 K increments. The results are tabulated in Table 4.2.

Table 4.2: Densities ρ and Excess Molar Volumes V_m^E of Binary Mixtures of MEA (1) + 3DMA1P (2) at Different Temperatures (T), Mass (w), Mole (x) Fractions and Atmospheric Pressure ($P = 0.1013 MPa$).[a]

T / K	ρ / kg/m^3	$V_m^E.10^{-6}$ / m^3/mol	T / K	ρ / kg/m^3	$V_m^E.10^{-6}$ / m^3/mol	T / K	ρ / kg/m^3	$V_m^E.10^{-6}$ / m^3/mol
				$w_1 = 0.1$, $x_1 = 0.160$				
298.15	893.6	-0.1000	318.15	877.56	-0.1069	338.15	861.17	-0.1121
303.15	889.62	-0.1037	323.15	873.5	-0.1083	343.15	857	-0.1145
308.15	885.61	-0.1029	328.15	869.41	-0.1096	348.15	852.81	-0.1170
313.15	881.6	-0.1055	333.15	865.3	-0.1109	353.15	848.59	-0.1195
				$w_1 = 0.2$, $x_1 = 0.299$				
298.15	905.51	-0.0918	318.15	889.48	-0.1003	338.15	873.13	-0.1103
303.15	901.53	-0.0954	323.15	885.43	-0.1031	343.15	868.96	-0.1124
308.15	897.53	-0.0962	328.15	881.35	-0.1055	348.15	864.78	-0.1158
313.15	893.52	-0.0988	333.15	877.25	-0.1080	353.15	860.57	-0.1190
				$w_1 = 0.3$, $x_1 = 0.421$				
298.15	917.73	-0.0993	318.15	901.73	-0.1113	338.15	885.4	-0.1230
303.15	913.76	-0.1038	323.15	897.68	-0.1140	343.15	881.26	-0.1280
308.15	909.77	-0.1060	328.15	893.61	-0.1174	348.15	877.09	-0.1321
313.15	905.76	-0.1086	333.15	889.52	-0.1208	353.15	872.89	-0.1360
				$w_1 = 0.4$, $x_1 = 0.529$				
298.15	925.55	0.3352	318.15	909.56	0.3385	338.15	893.26	0.3419
303.15	921.58	0.3349	323.15	905.51	0.3400	343.15	889.12	0.3420
308.15	917.59	0.3364	328.15	901.45	0.3402	348.15	884.96	0.3421
313.15	913.59	0.3370	333.15	897.36	0.3414	353.15	880.78	0.3415
				$w_1 = 0.5$, $x_1 = 0.628$				
298.15	934.52	0.6520	318.15	918.52	0.6683	338.15	902.22	0.6860
303.15	930.54	0.6556	323.15	914.48	0.6723	343.15	898.09	0.6893
308.15	926.56	0.6595	328.15	910.42	0.6765	348.15	893.93	0.6935
313.15	922.56	0.6632	333.15	906.33	0.6806	353.15	889.75	0.6971
				$w_1 = 0.6$, $x_1 = 0.717$				
298.15	944.89	0.8285	318.15	928.88	0.8532	338.15	912.58	0.8796
303.15	940.9	0.8349	323.15	924.85	0.8582	343.15	908.45	0.8855
308.15	936.92	0.8400	328.15	920.78	0.8651	348.15	904.29	0.8924
313.15	932.92	0.8457	333.15	916.7	0.8712	353.15	900.11	0.8990
				$w_1 = 0.71$, $x_1 = 0.806$				
298.15	960.16	0.7512	318.15	944.17	0.7737	338.15	927.89	0.7981
303.15	956.18	0.7571	323.15	940.14	0.7787	343.15	923.76	0.8045
308.15	952.2	0.7615	328.15	936.08	0.7848	348.15	919.61	0.8112
313.15	948.2	0.7671	333.15	932	0.7906	353.15	915.43	0.8177

Table 4.2 (Continued)

T	ρ	$V_m^E.10^{-6}$	T	ρ	$V_m^E.10^{-6}$	T	ρ	$V_m^E.10^{-6}$
K	kg/m^3	m^3/mol	K	kg/m^3	m^3/mol	K	kg/m^3	m^3/mol
				$w_1 = 0.8$, $x_1 = 0.871$				
298.15	975.11	0.5276	318.15	959.16	0.5412	338.15	942.92	0.5574
303.15	971.14	0.531	323.15	955.12	0.5455	343.15	938.8	0.5617
308.15	967.17	0.5335	328.15	951.08	0.5487	348.15	934.66	0.5661
313.15	963.17	0.5377	333.15	947.01	0.5527	353.15	930.5	0.5704
				$w_1 = 0.9$, $x_1 = 0.938$				
298.15	994.47	0.1617	318.15	978.54	0.1645	338.15	962.35	0.1678
303.15	990.51	0.1622	323.15	974.53	0.1643	343.15	958.25	0.1685
308.15	986.54	0.1622	328.15	970.49	0.1652	348.15	954.13	0.1692
313.15	982.55	0.1633	333.15	966.42	0.1669	353.15	949.98	0.1706
				$w_1 = 1.0$, $x_1 = 1.0$				
298.15	1011.9	0	318.15	995.94	0	338.15	979.78	0
303.15	1007.9	0	323.15	991.92	0	343.15	975.69	0
308.15	1003.9	0	328.15	987.89	0	348.15	971.58	0
313.15	999.94	0	333.15	983.84	0	353.15	967.45	0

[a]Standard uncertainties *u* are *u(T)=0.03 K*, *u(P) =2.0kPa*, *u(w)=0.01,* instrument standard uncertainty = *0.05kg/m*^{3}. The combined expanded uncertainty for density measurements $U_c(\rho) = 0.501 kg/m^3$ (95% level of confidence, *k = 2, Norm.*).

The densities were plotted against temperatures at different mass fractions (w_1) of MEA. This is shown in Figure 4.2. It can be observed from Figure 4.2 that there is a linear relationship between the densities and the temperatures. A gradual decrease of densities with increasing temperatures for all compositions can be seen. This is expected, because all substances tend to expand as they are heated, causing the same amount of mass to fill the space of a larger volume, and thus decreasing the density [32, pp. 10].

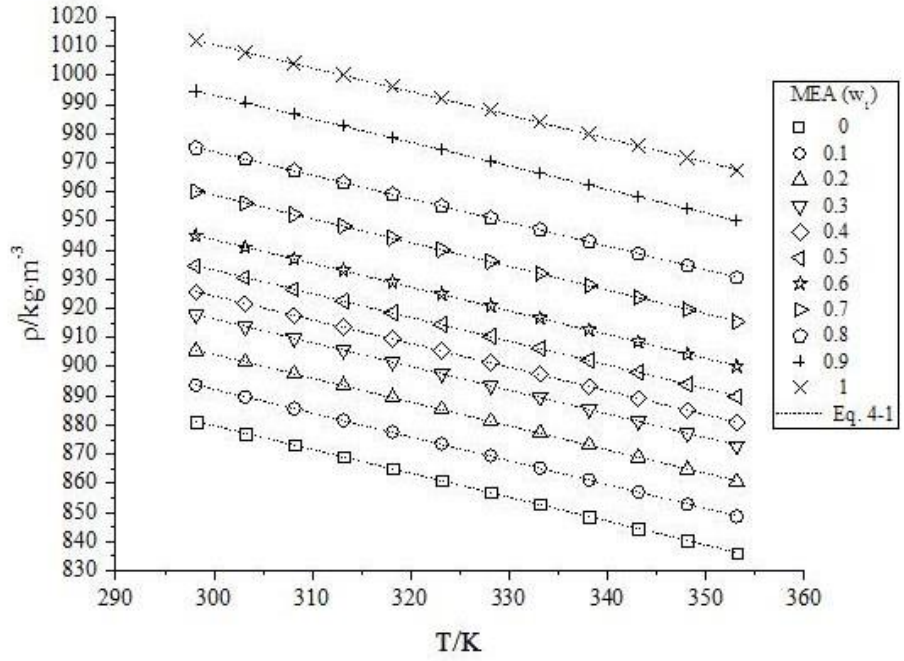

Figure 4.2: Densities of MEA (1) + 3DMA1P (2) binary system as a function of temperatures at different mass fractions (w_1) depicted with symbols. Correlations obtained from equation (4-1) between densities and temperatures are shown in dotted lines.

In addition, at any constant temperature, there is an increase in densities as the MEA content is increasing. This can be easily visualized in Figure 4.3. The density increase observed in Figure 4.3 as the MEA mass fraction is increasing while the temperature is kept constant, could be due to a significant degree of interactions between the molecules of MEA and 3DMA1P causing an important expansive behavior, that will result to density increase of the mixture [33].

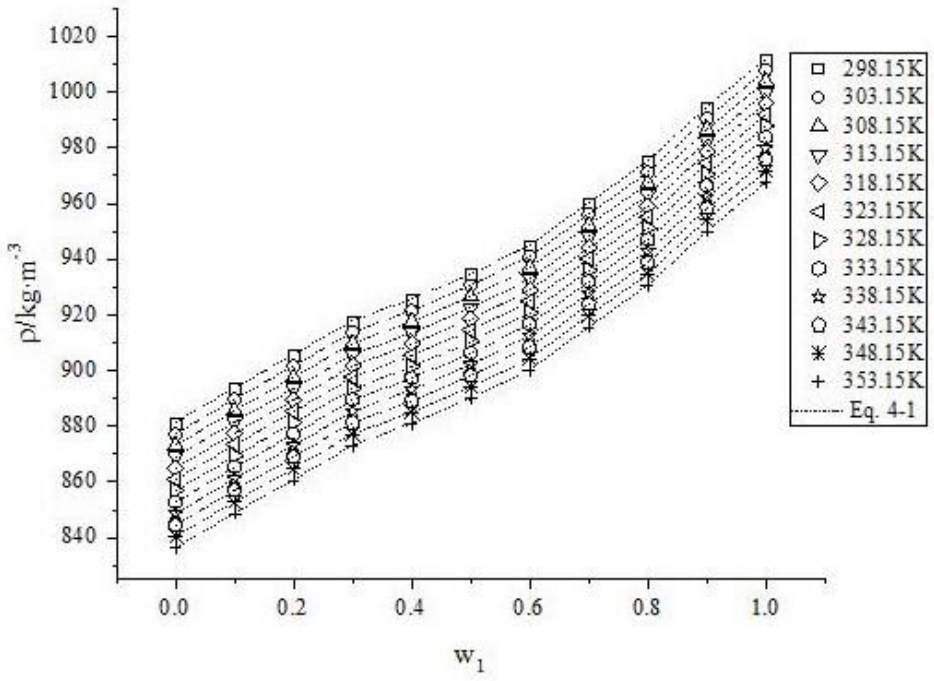

Figure 4.3: Densities of MEA (1) + 3DMA1P (2) binary system as a function of mass fractions (w_1) at various constant temperatures, depicted with symbols. Density values calculated as a function of temperature using equation (4-1) are shown in dotted lines.

It is trivial to understand that the reverse would be the case if instead the densities are plotted against the mass fractions of the second component (3DMA1P). A decrease in densities would be observed, with an increase in 3DMA1P content. It will then be reasonable to conclude that the behavior between the components' molecule is a contractive one.

The densities and temperatures of the binary system were correlated using equation (4-1).

$$\rho = A_0 + B_i \cdot T \qquad (4\text{-}1)$$

Where ρ is the density in $kg \cdot m^{-3}$, A_0 is the intercept of the *y*-axis, B_i is the slope of the straight line and *T* is the temperature in Kelvin. The values of A_0, B_i, coefficient of determination (R^2) and standard deviations calculated by equation (4-2), for the data are listed in Table 4.3.

$$\alpha = \left(\frac{\sum_{i=1}^{r} (\rho_{\exp,i} - \rho_{cal,i})^2}{r} \right)^{\frac{1}{2}} \qquad (4\text{-}2)$$

$\rho_{\exp,i}$ and $\rho_{cal,i}$ are respectively the experimental and corresponding calculated density of data point i; r is the number of experimental points.

From Table 4.3, we can see that the maximum standard deviation is *0.457kg/m^3*, which is within the experimental uncertainty for the binary system (*0.501kg/m^3*) and the coefficient of determination (R^2) values for all cases considered are very close to unity, which indicates that the correlated density values represent the measured values perfectly.

Table 4.3: Parameters of A_0, B_i, coefficient of determination R^2, and standard deviations, α for the linear correlation (Eq. 4-1) of density and temperature for MEA (1) + 3DMA1P (2) binary system at different values of MEA mass fraction w_1 and mole fraction x_1.

w_1	x_1	A_0	B_i	R^2	α kg/m^3
0.00	0.000	1125.34	-0.8184	0.9999	0.457
0.10	0.160	1137.68	-0.8180	0.9999	0.439
0.20	0.299	1149.19	-0.8166	0.9999	0.429
0.30	0.421	1160.90	-0.8149	0.9999	0.409
0.40	0.529	1168.35	-0.8137	0.9999	0.387
0.50	0.628	1177.31	-0.8137	0.9999	0.384
0.60	0.717	1187.69	-0.8138	0.9999	0.387
0.70	0.806	1202.67	-0.8128	0.9999	0.382
0.80	0.871	1217.00	-0.8107	0.9999	0.365
0.90	0.938	1235.70	-0.8086	1.0000	0.341
1.00	1.000	1252.64	-0.8071	1.0000	0.307

As part of this research work, the experimental values of density for the aqueous ternary (MEA + 3DMA1P + H_2O) system were measured at various mass fractions of MEA and 3DMA1P, within the temperature range of (298.15 - 353.15) K. The measured densities and the corresponding values of excess molar volumes are listed in Table 4.4.

Table 4.4: Experimental Densities ρ and Excess Molar Volumes V_m^E of MEA (1) + 3DMA1P (2) + H_2O (3) Ternary Systems at Different Temperatures (T), Mass (w), Mole (x) fractions and Atmospheric Pressure ($P = 0.1013MPa$).[a]

T / K	ρ / kg/m^3	$V_m^E.10^{-6}$ / m^3/mol	T / K	ρ / kg/m^3	$V_m^E.10^{-6}$ / m^3/mol	T / K	ρ / kg/m^3	$V_m^E.10^{-6}$ / m^3/mol
				$w_1 = 0.30$, $w_2 = 0$, $x_1 = 0.113$, $x_2 = 0$				
298.15	1010.52	-0.2043	318.15	1000.62	-0.1998	338.15	987.46	-0.1682
303.15	1008.25	-0.2026	323.15	997.62	-0.1947	343.15	984.25	-0.1684
308.15	1005.87	-0.2022	328.15	994.3	-0.1849	348.15	981.04	-0.1712
313.15	1003.34	-0.2016	333.15	990.91	-0.1760	353.15	977.77	-0.1750
				$w_1 = 0$, $w_2 = 0.30$, $x_1 = 0$, $x_2 = 0.070$				
298.15	983.91	-0.6272	318.15	971.75	-0.5900	338.15	957.97	-0.5625

Table 4.4 (Continued)

T	ρ	$V_m^E.10^{-6}$	T	ρ	$V_m^E.10^{-6}$	T	ρ	$V_m^E.10^{-6}$
K	kg/m^3	m^3/mol	K	kg/m^3	m^3/mol	K	kg/m^3	m^3/mol
303.15	981.03	-0.6166	323.15	968.45	-0.5825	343.15	954.29	-0.5566
308.15	978.05	-0.6071	328.15	965.04	-0.5752	348.15	950.52	-0.5509
313.15	974.95	-0.5981	333.15	961.56	-0.5689	353.15	946.66	-0.5454
			$w_1 = 0.24$, $w_2 = 0.06$, $x_1 = 0.091$, $x_2 = 0.013$					
298.15	1005.18	-0.2885	318.15	995.09	-0.2841	338.15	983.09	-0.2843
303.15	1002.83	-0.2861	323.15	992.03	-0.2787	343.15	979.83	-0.2848
308.15	1000.35	-0.2845	328.15	989.13	-0.2798	348.15	976.47	-0.2854
313.15	997.68	-0.2817	333.15	986.14	-0.2814	353.15	973.01	-0.2861
			$w_1 = 0.18$, $w_2 = 0.12$, $x_1 = 0.069$, $x_2 = 0.027$					
298.15	999.89	-0.3734	318.15	989.32	-0.3625	338.15	976.9	-0.3571
303.15	997.41	-0.3693	323.15	986.38	-0.361	343.15	973.62	-0.3583
308.15	994.81	-0.366	328.15	983.32	-0.3594	348.15	970.15	-0.3574
313.15	991.96	-0.3601	333.15	980.14	-0.3576	353.15	966.58	-0.3565
			$w_1 = 0.12$, $w_2 = 0.18$, $x_1 = 0.046$, $x_2 = 0.041$					
298.15	994.76	-0.462	318.15	983.78	-0.4459	338.15	970.82	-0.4317
303.15	992.15	-0.456	323.15	980.41	-0.435	343.15	967.33	-0.4288
308.15	989.34	-0.4488	328.15	975.79	-0.3961	348.15	963.6	-0.4225
313.15	986.18	-0.4365	333.15	973.64	-0.4208	353.15	960.23	-0.4277
			$w_1 = 0.06$, $w_2 = 0.24$, $x_1 = 0.023$, $x_2 = 0.055$					
298.15	989.26	-0.5427	318.15	977.84	-0.52	338.15	964.43	-0.4984
303.15	986.25	-0.5279	323.15	974.62	-0.5137	343.15	958.8	-0.4414
308.15	983.95	-0.5342	328.15	971.35	-0.509	348.15	953.19	-0.3865
313.15	980.17	-0.5075	333.15	967.97	-0.5044	353.15	948.88	-0.3675
			$w_1 = 0.50$, $w_2 = 0$, $x_1 = 0.228$, $x_2 = 0$					
298.15	1020.83	-0.4456	318.15	1008.52	-0.4289	338.15	995.05	-0.4241
303.15	1017.86	-0.4397	323.15	1005.26	-0.4271	343.15	991.5	-0.4239
308.15	1014.82	-0.4353	328.15	1001.93	-0.4257	348.15	987.86	-0.4234
313.15	1011.7	-0.4314	333.15	998.52	-0.4246	353.15	984.13	-0.4226
			$w_1 = 0$, $w_2 = 0.50$, $x_1 = 0$, $x_2 = 0.149$					
298.15	970.57	-1.1848	318.15	955.09	-1.1016	338.15	938.77	-1.0381
303.15	966.77	-1.1616	323.15	951.1	-1.0847	343.15	934.54	-1.0241
308.15	962.93	-1.14	328.15	947.05	-1.0686	348.15	930.24	-1.0102
313.15	959.05	-1.1206	333.15	942.94	-1.0531	353.15	925.89	-0.997
			$w_1 = 0.40$, $w_2 = 0.10$, $x_1 = 0.186$, $x_2 = 0.028$					
298.15	1011.2	-0.6071	318.15	998.16	-0.5779	338.15	984	-0.5612
303.15	1008.03	-0.5977	323.15	994.73	-0.5731	343.15	980.28	-0.558
308.15	1004.81	-0.5902	328.15	991.22	-0.5686	348.15	976.48	-0.5549
313.15	1001.53	-0.5838	333.15	987.65	-0.5649	353.15	972.63	-0.5525
			$w_1 = 0.30$, $w_2 = 0.20$, $x_1 = 0.142$, $x_2 = 0.056$					

Table 4.4 (Continued)

T	ρ	$V_m^E.10^{-6}$	T	ρ	$V_m^E.10^{-6}$	T	ρ	$V_m^E.10^{-6}$
K	kg/m^3	m^3/mol	K	kg/m^3	m^3/mol	K	kg/m^3	m^3/mol
298.15	1001.86	-0.7759	318.15	988.25	-0.7374	338.15	973.39	-0.7073
303.15	998.43	-0.7608	323.15	984.62	-0.7286	343.15	969.6	-0.704
308.15	995.24	-0.7559	328.15	980.95	-0.7212	348.15	965.73	-0.7006
313.15	991.73	-0.7447	333.15	977.2	-0.714	353.15	961.78	-0.6971
			$w_1 = 0.20$, $w_2 = 0.30$, $x_1 = 0.097$, $x_2 = 0.086$					
298.15	992.86	-0.9541	318.15	978.52	-0.9004	338.15	963.23	-0.8638
303.15	989.3	-0.9367	323.15	974.79	-0.8902	343.15	959.27	-0.857
308.15	985.59	-0.918	328.15	971	-0.8809	348.15	955.14	-0.8472
313.15	982.19	-0.9118	333.15	967.15	-0.8722	353.15	951.04	-0.8408
			$w_1 = 0.10$, $w_2 = 0.40$, $x_1 = 0.049$, $x_2 = 0.116$					
298.15	981.71	-1.0701	318.15	966.73	-1.0003	338.15	950.6	-0.9402
303.15	978.09	-1.0519	323.15	962.64	-0.9794	343.15	946.24	-0.9211
308.15	974.09	-1.0248	328.15	959.09	-0.979	348.15	941.84	-0.9029
313.15	970.49	-1.0135	333.15	954.99	-0.9632	353.15	937.17	-0.8779
			$w_1 = 0.05$, $w_2 = 0.45$, $x_1 = 0.025$, $x_2 = 0.132$					
298.15	975.84	-1.118	318.15	960.11	-1.0249	338.15	943.96	-0.9649
303.15	971.9	-1.0898	323.15	956.38	-1.016	343.15	938.41	-0.9048
308.15	968.13	-1.0702	328.15	952.24	-0.9965	348.15	935.77	-0.9475
313.15	964.33	-1.0529	333.15	948.49	-0.9926	353.15	929.74	-0.8749
			$w_1 = 0.45$, $w_2 = 0.05$, $x_1 = 0.207$, $x_2 = 0.014$					
298.15	1018.14	-0.5843	318.15	1005.6	-0.5667	338.15	991.92	-0.5618
303.15	1015.08	-0.5773	323.15	1002.26	-0.5641	343.15	988.32	-0.5617
308.15	1011.96	-0.572	328.15	998.85	-0.5619	348.15	984.64	-0.5616
313.15	1008.71	-0.5659	333.15	995.47	-0.5631	353.15	980.89	-0.5618

[a]Standard uncertainties u are u(T)=0.03 K, u(P) =2.0kPa, u(w)=0.01, instrument standard uncertainty = 0.05kg/m3. The combined standard uncertainty for density measurements $U_c(\rho) = 0.501 kg/m^3$(95% level of confidence, $k = 2$, *Norm.).*

The densities of the ternary systems were plotted against temperatures for all the mass fractions considered, as shown in Figure 4.4. A linear relationship can be observed in Figure 4.4, where the densities are decreasing gradually as temperature is increasing for all cases, as expected. The reason [32, pp. 10] for this behavior is the same to the one discussed for the binary systems (MEA + 3DMA1P).

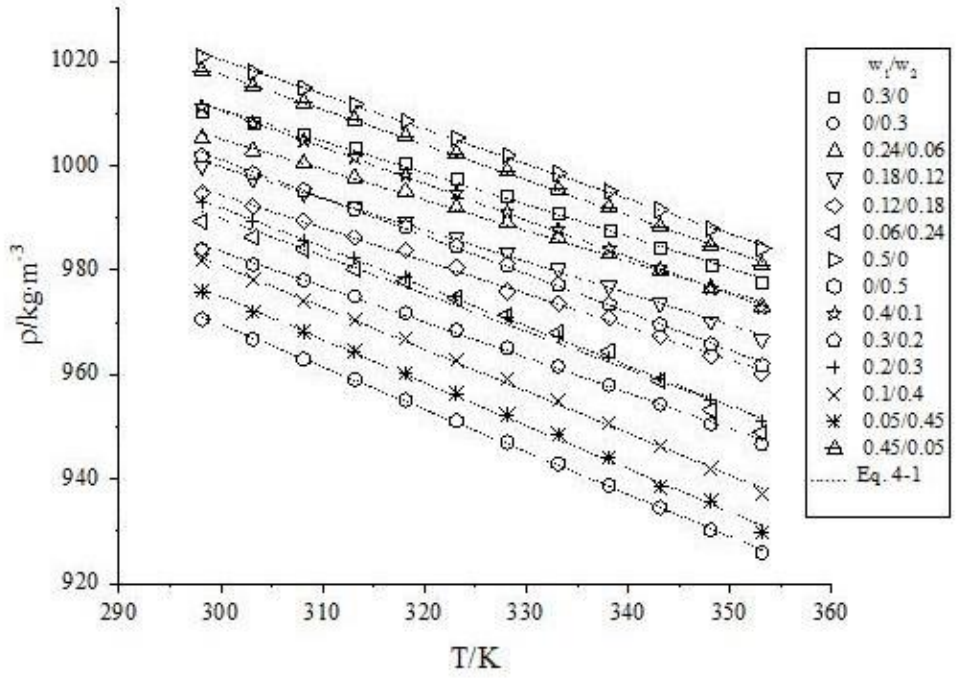

Figure 4.4: Densities of MEA (1) + 3DMA1P (2) + H_2O (3) ternary system as a function of temperatures at different mass fractions (w_1/w_2) depicted with symbols. Correlations obtained from equation (4-1) between densities and temperatures are shown in dotted lines.

It can be observed (Table 4.4 and Figure 4.4) within the range of temperature considered, that the highest density values were achieved for the 0.5/0/0.5 ($x_1/x_2/x_3$) binary solution and are between (1020.83 – 984.13) $kg{\cdot}m^{-3}$, while the lowest density values which are between (970.57 – 925.89) $kg{\cdot}m^{-3}$ can be seen for the 0/0.5/0.5 binary solution. This behavior makes scientific sense, considering the fact that at constant temperature, the densities of pure MEA are higher than the densities of pure 3DMA1P, and as such, the same trend should follow when two different solutions contain the same amount of MEA in one solution and 3DMA1P in the other solution. This same behavior is observed when comparing the 0.3/0/0.7 and 0/0.3/0.7 systems as shown in Figure 4.4.

A three dimensional scatter plots for the densities of the ternary systems as a function of mass fraction (w_1) and temperature are shown in Figure 4.5. Looking at Figure 4.5(a) and Figure 4.5(b), it is interesting to notice the systematic reduction of the densities as the content of MEA is reduced, corresponding to an increase in 3DMA1P content, for both the aqueous 50% and 30% total amine concentrations. This behavior could be attributed to the resulting contraction which takes place due to significant molecular interactions between the MEA and 3DMA1P, as the content is being reduced and increased respectively [33].

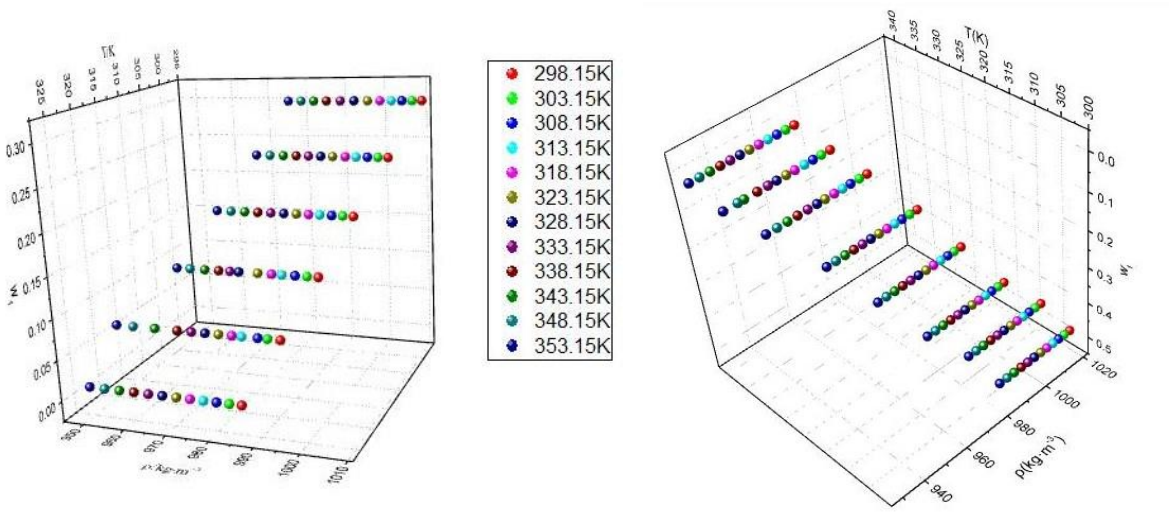

(a) (b)

Figure 4.5: Three dimensional scatter for densities of MEA (1) +3DMA1P (2) + H_2O (3) as a function of mass fraction (w_1), temperature T (in Kelvin), depicted by symbols; (a) 0.3 and (b) 0.5 total amine mass fraction, w present in the aqueous ternary solutions.

The linear relationship between densities and temperatures were correlated using equation (4-1). Table 4.5 shows the values for A_0, B_i, coefficient of determination (R^2) and standard deviations α calculated by equation (4-2) for the systems considered. It can be seen from Table 4.5 that all the standard deviations are within the experimental uncertainty (*2.082kg/m^3*) except for the 0.05/0.45 system (*2.29 kg/m^3*) which is very close to the uncertainty limit. Nevertheless, taking note of this observation, and the fact that the coefficients of determination (R^2) are close to unity, we can conclude that the predicted density values and the measured values are in very good agreement.

Table 4.5: Parameters of A_0, B_i and coefficient of determination R^2, for the linear correlation of density and temperature for MEA(1) + 3DMA1P(2) + H_2O(3) ternary system at different values of MEA and 3DMA1P mass fractions w and mole fractions x.

w_1/w_2	x_1/x_2	A_0	B_i	R^2	α/ kg/m^3
0.30/0.00	0.113/0.000	1192.90	-0.6072	0.9959	
0.24/0.06	0.091/0.013	1180.78	-0.5856	0.9971	1.78
0.18/0.12	0.069/0.027	1181.41	-0.6056	0.9972	1.89
0.12/0.18	0.046/0.041	1183.74	-0.6313	0.9976	1.93

Table 4.5 (Continued)					
0.06/0.24	0.023/0.055	1205.80	-0.7198	0.9834	1.84
0.00/0.30	0.000/0.070	1186.97	-0.6780	0.9981	
0.50/0.00	0.228/0.000	1220.31	-0.6668	0.9989	1.35
0.45/0.05	0.207/0.014	1220.35	-0.6762	0.9990	1.03
0.40/0.10	0.186/0.028	1220.88	-0.7011	0.9990	1.30
0.30/0.20	0.142/0.056	1219.96	-0.7295	0.9992	1.21
0.20/0.30	0.097/0.086	1219.45	-0.7583	0.9993	1.19
0.10/0.40	0.049/0.116	1222.05	-0.8038	0.9985	1.85
0.05/0.45	0.025/0.132	1222.76	-0.8260	0.9978	2.29
0.00/0.50	0.000/0.149	1213.11	-0.8118	0.9996	1.29

4.1.2 Excess molar volumes

The experimental density values were used to calculate the excess molar volumes for the binary and the ternary systems. The excess molar volumes were calculated from equation 4-3. The calculated excess molar volumes of the binary and the ternary systems are listed in Table 4.2 and Table 4.4 respectively. The values for the binary system, along with those sourced from the literature [21, 23] were utilized to predict the excess molar volumes of the ternary system.

$$V_m^E = \sum_{i=1}^{n} x_i M_i \left[(1/\rho) - (1/\rho_i)\right] \qquad (4\text{-}3)$$

V_m^E is the excess molar volume; n is the number of components; x_i, M_i and ρ_i are respectively the mole fraction, molar mass and pure density of component i in the mixture; ρ is the measured density of the mixture.

In addition, equation (4-4) which is the Redlich-Kister [6] (RK) polynomial equation was used to fit the excess molar volumes for the MEA (1) + 3DMA1P (2) binary mixtures.

$$V_{ij}^E = x_i x_j \sum_{k=0}^{p} A_k \left(2x_i - 1\right)^k \qquad (4\text{-}4)$$

A_k represents the adjustable parameters; x_i and x_j are respectively the mole fraction of component i and j; $p+1$ is the number of adjustable parameters.

A statistical test which is used to compare models that has been fitted to data set, and choose the statistical model that best fits the data sampled, is known as the *F*-test [34]. The F-test was employed to select the order of the RK polynomial that best fit the excess molar volumes of the

binary systems. A model comparison of the second, third and fourth order RK polynomial was performed using the F statistic equation, represented by equation (4-5). If the probability value is higher than the critical *F* value [1], then the first model is statistically better than the second. If on the other side, the probability value is lower than the critical *F* value, then the second model is statistically better [34].

$$F = \frac{(SS_1 - SS_2)/(df_1 - df_2)}{SS_2 / df_2} \qquad (4\text{-}5)$$

SS_1 and SS_2 are respectively the residual sum of squares for the first and second model compared, while df_1 and df_2 are the degrees of freedom of first and second model respectively.

Comparing the probability values with the critical values of *F,* shows that the fourth order (RK-4) polynomial best fit the data within the range considered. Table 4.6 shows the calculated values for the *F*-test at 298.15 K.

Table 4.6: F-test for the comparison of RK polynomials of order 2,3, and 4 showing the residual sum of squares of first (SS_1) and second (SS_2) model, degrees of freedom of first (df_1) and second (df_2) model, F values, probability (p) values, critical F (F-crit.) and the best fit for the plot of binary mixtures of MEA + 3DMA1P at 298.15 K.

Models	***SS_1***	***SS_2***	***df_1***	***df_2***	***F***	***p-value***	***F-crit.***	***Best***
RK-2, RK-3	0.1245	0.0326	8	7	19.7171	0.0030	0.1112	RK-3
RK-3, RK-4	0.0326	0.0105	7	6	12.7349	0.0118	0.1476	RK-4

Since the RK fourth order (RK-4) is the best fit for the data at 293.18 K, we can extend this conclusion to other temperatures because there is no significant changes in the excess molar volumes with temperature, as illustrated in Figure 4.6. The adjustable parameters of the fits at each temperature are given in Table 4.6. The levels of confidence R^2, and the corresponding root mean square deviations α, calculated from equation (4-6) are also shown in Table 4.7.

[1] The values are functions of calculated *F*, and can be computed in MATLAB using the 'fcdf' function.

$$\alpha = \left(\frac{\sum_{i=1}^{r} (V_{\exp,i}^{E} - V_{cal,i}^{E})^{2}}{r} \right)^{\frac{1}{2}} \qquad (4\text{-}6)$$

$V_{\exp,i}^{E}$ and $V_{cal,i}^{E}$ are respectively the experimental and calculated excess molar volume, equation (4-4) of data point i ; r is the number of experimental points.

Table 4.7: Redlich-Kister fourth order parameters A_p for MEA + 3DMA1P mixtures at different temperatures. The levels of confidence R^2 of the lines and root mean square deviations α are also given.

T/K	A_0	A_1	A_2	A_3	A_4	R^2	α
298.15	0.7348	6.6018	7.1682	-5.5652	-9.2013	0.9921	0.0308
303.15	0.7274	6.6694	7.2695	-5.6110	-9.3625	0.9921	0.0311
308.15	0.7278	6.7218	7.3354	-5.6943	-9.4295	0.9920	0.0314
313.15	0.7255	6.7759	7.4063	-5.7227	-9.5296	0.9921	0.0316
318.15	0.7258	6.8410	7.5002	-5.7850	-9.6608	0.9921	0.0319
323.15	0.7253	6.9019	7.5514	-5.8503	-9.7209	0.9920	0.0323
328.15	0.7213	6.9676	7.6504	-5.9190	-9.8481	0.9921	0.0324
333.15	0.7195	7.0318	7.7129	-5.9837	-9.9058	0.9920	0.0328
338.15	0.7180	7.1028	7.8304	-6.0479	-10.0652	0.9922	0.0327
343.15	0.7100	7.1621	7.9515	-6.0860	-10.2321	0.9920	0.0334
348.15	0.7043	7.2336	8.0542	-6.1457	-10.3711	0.9921	0.0336
353.15	0.6971	7.2981	8.1603	-6.1900	-10.5094	0.9921	0.0338

The excess molar volumes of the binary system, at different temperatures were plotted against the mole fractions of components. These are shown in Figure 4.6.

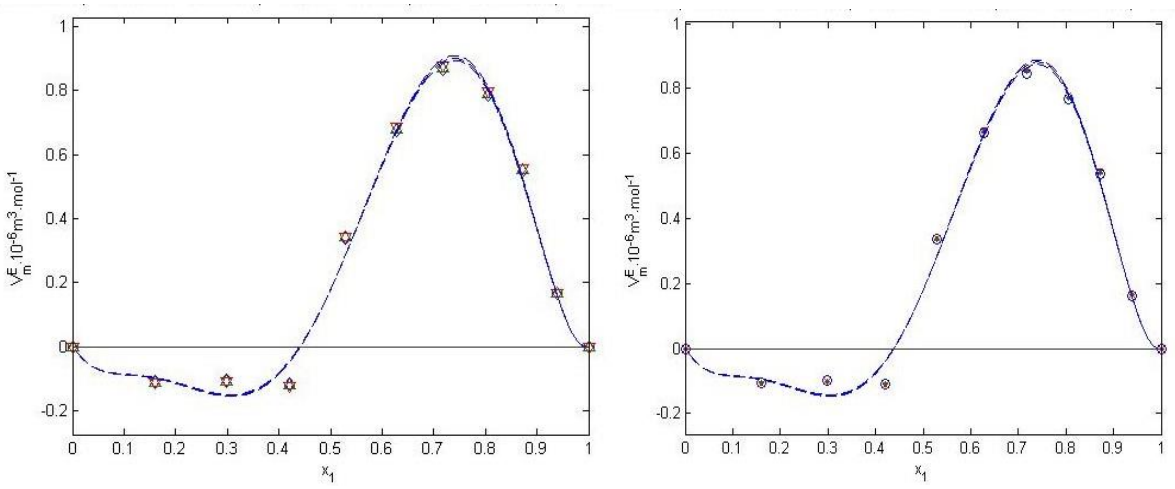

(a) (b)

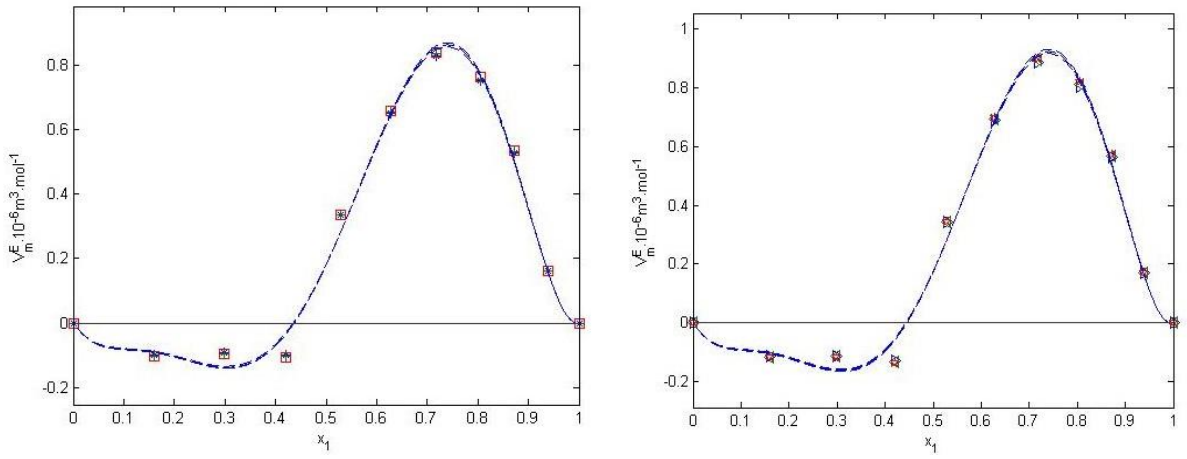

(c) (d)

*Figure 4.6: Experimental values of excess molar volumes V_m^E for MEA (1) + 3DMA1P (2) binary mixtures at different temperatures: (**a**) 298.15 (*), 303.15 (+), 308.15 (o); (**b**) 313.15 (o), 318.15 (.), 323.15 (x); (**c**) 328.15 (□), 333.15 (△), 338.15 (▽); (**d**) 343.15 (◁), 348.15 (▷), 353.15 (☆) and the broken lines were calculated from equation (4-3).*

It can be seen from Figure 4-6 that at all temperature ranges considered, the curves exhibit a similar behavior which is an S-shape, having a negative value as minimum and a positive value as maximum. An inversion of sign for V_m^E can be observed within $x_1 \approx 0.45$.

The negative values of V_m^E in the lower region is most likely due to two types of interaction [35, 36]: (**1**) chemical or charge transfer interactions, leading to the formation of hydrogen bonds between the hydroxyl group and amidogen (NH_2) present in the molecules of MEA and 3DMA1P, resulting to a negative (-) contribution. (**2**) Structural interaction, which is the accommodation of MEA and 3DMA1P molecules into each other's structure due to difference in shape and size, leading to volumetric contraction and resulting to a negative contribution. However, as the MEA content is about becoming rich in the mixtures ($x_1 \geq 0.45$), the physical interactions which most likely, is due to repulsive forces or weak dipole-dipole intermolecular interaction between MEA and 3DMA1P predominates the structural and chemical interactions, and thus resulting to the positive trend observed in the upper region. In other words, the presence of a larger amount of MEA in the mixture has the tendency to change the sign of V_m^E from negative to positive [37, 38].

In order to estimate thermodynamic properties of a ternary system from the properties of the constituent binary systems using predictive models, this would mean that the required data of the binary systems should be available. Three different binary systems, comprising two components from the three components in a ternary system will be required to predict a ternary system property [36].

As part of this work to predict the excess molar volumes of a ternary system, the experimental results of the binary system (MEA + 3DMA1P) in this work were used to study the ternary system (MEA + 3DMA1P + H_2O). However, the remaining two binary systems required were sourced from literature.

The excess molar volumes of the binary (3DMA1P + H_2O) system were sourced from the work of [23], while that of the (MEA + H_2O) aqueous solution were sourced from the work of [21].

The experimental excess molar volumes for the MEA + 3DMA1P + H_2O systems were listed alongside the densities in Table 4.4. It can be seen from Table 4.4 that all the values are negative over the entire compositions. This behavior can be qualitatively explained by the strong ion-dipole interactions and packing effect between MEA, 3DMA1P and H_2O dominating over dissociation of intermolecular hydrogen bonds in MEA and 3DMA1P [21, 23, 39, 40].

The ternary V_m^E data were correlated using equation (4-7), which is the Nagata-Tamura [41] equation.

$$V_{m,123}^E = V_{m,12}^E + V_{m,13}^E + V_{m,23}^E + x_1x_2x_3RT(B_0 - B_1x_1 - B_2x_2 - B_3x_1^2 - B_4x_2^2 - B_5x_1x_2 - B_6x_1^3 - B_7x_2^3 + B_8x_1^2x_2) \quad (4\text{-}7)$$

Where $V_{m,ij}^E$ was calculated using equation (4-4) with the fitted parameters; x_1, x_2 and x_3 are respectively the mole fractions of MEA, 3DMA1P and H_2O. *R* is the molar gas constant and *T* is the temperature in Kelvin. $B_0, B_1 \ldots\ldots B_8$ are the adjustable parameters for the ternary contribution which were calculated by least square fitting.

The fitted parameters and the corresponding α for equation (4-7), calculated according to equation (4-6) are listed in Table 4.8. The $V_{m,123}^E$ values at 348.15K and 353.15K could not be correlated because of the unavailability of the binary data (H_2O + 3DMA1P) at the temperatures.

Table 4.8: Parameters B_i of the correlation, Eq. (4-7) and the corresponding standard deviations α at different temperatures for MEA (1) + 3DMA1P (2) + H2O (3) ternary system.

T/K	B_0	B_1	B_2	B_3	B_4	B_5	B_6	B_7	B_8	α
298.15	4.67	329.7	-111.7	-3738.4	3977.3	-3414.5	10455.7	-20274.4	24610.0	0.0210
303.15	4.63	311.6	-98.6	-3503.1	3687.9	-3222.2	9768.1	-18932.6	22984.4	0.0215
308.15	4.84	333.3	-109.3	-3762.5	3987.9	-3452.2	10506.1	-20404.9	24743.5	0.0209
313.15	4.43	308.7	-102.7	-3491.7	3704.5	-3195.5	9756.8	-18919.5	22964.2	0.0212
318.15	5.05	322.4	-94.1	-3588.5	3740.8	-3332.0	9970.0	-19369.2	23476.3	0.0214
323.15	4.59	326.0	-111.2	-3699.5	3943.3	-3379.2	10348.6	-20094.8	24368.4	0.0207
328.15	4.52	304.3	-97.1	-3419.6	3621.5	-3153.9	9531.3	-18593.2	22475.8	0.0222
333.15	4.85	336.0	-111.1	-3796.4	4032.9	-3482.6	10602.6	-20621.4	24979.6	0.0214
338.15	4.94	334.3	-106.9	-3761.3	3973.0	-3460.9	10489.9	-20385.0	24703.5	0.0205
343.15	5.74	314.6	-66.2	-3390.5	3379.4	-3225.8	9310.2	-17995.3	21867.7	0.0207

In different angles of view, Figure 4.7 shows selected 3D mesh plots (298.15K, 323.15K and 343.15K) of the excess molar volumes calculated by using equation (4-6) as a function of the mole fraction of MEA (1) and 3DMA1P (2). It can be deduced from Figure 4.7 that there is no significant change for $V^E_{m,123}$ with increase in temperature. It is important to note that although the model have a good representation of the experimental $V^E_{m,123}$ ternary data considering the standard deviations, but however, large positive values of $V^E_{m,123}$ was observed as the mole fraction of the components (x_1 and x_2) becomes larger at about $x_i \approx 0.2$, well above the maximum mole fractions considered in this work. It is very difficult to find an explanation for this behavior, but, the best possible explanation is most likely from the nature of the model itself, as similarly observed from the work reported by Jelena et al. [36].

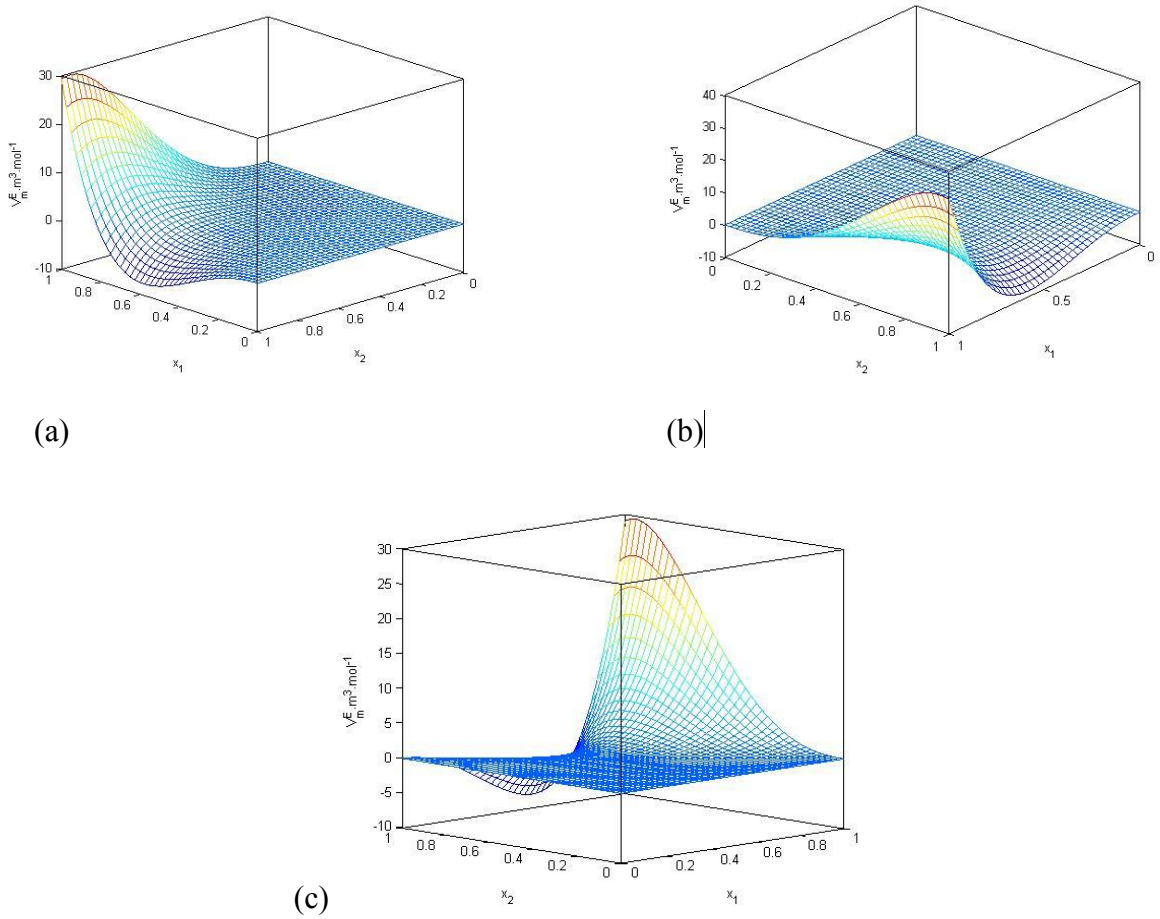

*Figure 4.7: 3 dimensional plots of the excess molar volumes, $V^{E}_{m,123}$ for MEA (1) +3DMA1P (2) + H_2O (3) ternary system calculated using Eq. (4-6) at **(a)** 298.15K, **(b)** 323.15K and **(c)** 343.15K.*

In the absence of ternary data, several semi-empirical models have been developed by scientists to predict ternary properties from the available constituent binary properties. This is because the effect of mixing is generally a drawback in predicting ternary thermo-physical properties from pure components, which explains why those methods are not so reliable. Therefore, it is necessary to have more extensive study in using the constituent binary properties to estimate the ternary properties [42].

As part of this project, the MEA + 3DMA1P + H_2O ternary $V^{E}_{m,123}$ data was predicted from the MEA + H_2O and 3DMA1P + H_2O binary systems available in the literature [21, 23], and the MEA + 3DMA1P binary systems measured in this work. The predicted ternary $V^{E}_{m,123}$ values were compared with that of the experimental values. The Radojkovic et al. [43], Kohler [44]

and Jacob-Fitzner [45] models were used to predict the ternary excess molar volumes $V^E_{m,123}$. The expressions of these models are respectively given as equation (4-8), equation (4-9) and equation (4-10).

$$V^E_{ijk} = \sum_{j>1} V^E_{ij}(\bar{x}_i, \bar{x}_j) \tag{4-8}$$

V^E_{ij} is the excess molar volume of the corresponding binary components *i* and *j*. The binary contributions were evaluated at the mole fractions $\bar{x}_i = x_i$ and $\bar{x}_j = x_j$.

$$V^E_{ijk} = \sum_{j>i} (x_i + x_j)^2 V^E_{ij}(\bar{x}_i, \bar{x}_j) \tag{4-9}$$

V^E_{ij} is the excess molar volume of the corresponding binary components *i* and *j*. The binary contributions were evaluated at the mole fractions $\bar{x}_i = \dfrac{x_i}{x_i + x_j}$ and $\bar{x}_j = 1 - \bar{x}_i$.

$$V^E_{123} = \frac{x_1 x_2}{(x_1 + x_3/2)(x_2 + x_3/2)} V^E_{12}(\bar{x}_1, \bar{x}_2) + \frac{x_1 x_3}{(x_1 + x_2/2)(x_3 + x_2/2)} V^E_{13}(\bar{x}_1, \bar{x}_3)$$

$$+ \frac{x_2 x_3}{(x_2 + x_1/2)(x_3 + x_1/2)} V^E_{23}(\bar{x}_2, \bar{x}_3) \tag{4-10}$$

V^E_{ij} is the excess molar volume of the corresponding binary components *i* and *j*. The binary contributions were evaluated at the mole fractions $\bar{x}_i = (1 + x_i - x_j)/2$ and $\bar{x}_j = 1 - \bar{x}_i$.

The predicted values of $V^E_{m,123}$ estimated by these models, compared with the experimental values at different temperatures are available in Appendix D. The corresponding root mean square deviations α, calculated by equation (4-11) are listed in Table 4.9.

$$\alpha = \left(\frac{\sum_{i=1}^{r} (V^E_{\exp,i} - V^E_{prd,i})^2}{r} \right)^{\frac{1}{2}} \tag{4-11}$$

$V^E_{\exp,i}$ and $V^E_{prd,i}$ are respectively the experimental and corresponding predicted excess molar volume of data point *i* ; *r* is the number of experimental points.

Table 4.9: Excess molar volume root mean square deviations, α for predictive models at different temperatures T.

T/K	$\alpha \cdot 10^{-6} / m^3 \cdot mol^{-1}$	T/K	$\alpha \cdot 10^{-6} / m^3 \cdot mol^{-1}$	T/K	$\alpha \cdot 10^{-6} / m^3 \cdot mol^{-1}$
Radojkovic et al.		***Kohler***		***Jacob-Fitzner***	
298.15	0.0828	298.15	0.0848	298.15	0.0935
303.15	0.0818	303.15	0.0842	303.15	0.0923
308.15	0.0799	308.15	0.0828	308.15	0.0904
313.15	0.0807	313.15	0.0838	313.15	0.0903
318.15	0.0826	318.15	0.0862	318.15	0.0923
323.15	0.0814	323.15	0.0851	323.15	0.0911
328.15	0.0830	328.15	0.0870	328.15	0.0919
333.15	0.0853	333.15	0.0895	333.15	0.0944
338.15	0.0831	338.15	0.0873	338.15	0.0925
343.15	0.0809	343.15	0.0855	343.15	0.0914

From Table 4.9, we can see that at any constant temperature, the Radojkovic et al. model is the most adequate of the three models in predicting the experimental excess molar volumes as its standard deviations are the lowest. Kohler model comes second, while the Jacob-Fitzner prediction have higher deviations.

4.2 Ternary system (MDEA + PZ + H_2O)

As a second set of experiment, the densities of the ternary amine solution (MDEA + PZ + H_2O) at different amine concentrations and temperature range of (293.15-363.15) K, at 5K increment were measured. The measured densities are presented in Appendix E. All the experimentally determined density data were modelled in a non-dimensional form with the least square fitting and the Orthorgonal Distance Regression (ODR) iteration algorithm, using a second order polynomial function as in the work of Arunkumar and Syamalendu [46]. The model equation is a function of temperature and total amine mass fraction and is depicted as equation (4-12).

$$\rho = \sum_{i=0}^{2} \left[A_i W^i + B_i W^i T + C_i W^i T^2 \right] \qquad (4\text{-}12)$$

The density of the mixture is denoted by ρ ; T is the temperature in Kelvin; A, B and C are the correlation parameters corresponding to i, and W is the total amine mass fraction present in the solution, calculated by equation (4-13).

$$W = \sum_{i=1}^{2} w_i \qquad (4\text{-}13)$$

w is the mass fraction of i, each individual amine (MDEA and PZ) present in the solution.

The values for the correlation parameters and standard deviation α, calculated by equation (4-2) are listed in Table 4.10.

Interestingly, this single equation (equation (4-12)) was able to correlate all the density data with a standard deviation of *0.0094 kg/m^3* which is well below the experimental combined expanded uncertainty (*0.414 kg/m^3)* of the ternary system, and R^2 value of 1, as shown in Table 4.10. This indicate that the density data is in excellent agreement with the model.

Table 4.10: Fitted Parameters of Equation 4-12, Coefficient of Determination R^2, and Standard Deviation α for Density Correlations for The Ternary Systems MDEA + PZ + H_2O.

	A_i	B_i	C_i
i = 0	826.92	1.25832	-0.0025
i = 1	290.919	0.00201	-0.0016
i = 2	446.198	-3.6646	0.00642
R^2		1	
α		0.0094 kg/m^3	

Figure 4.8(a), (b) and (c) shows the densities of the ternary solutions as a function of temperature for the mass fractions of PZ. It can be seen from Figure 4.8 that the densities of MDEA + PZ +H_2O as expected, decrease as the temperature increases [32, pp. 10] and increase as the mass fraction of PZ increases in the solution. This behavior can be observed as the PZ content increases in all the constant MDEA/H_2O compositions considered (30/70, 40/60, and 50/50) %.

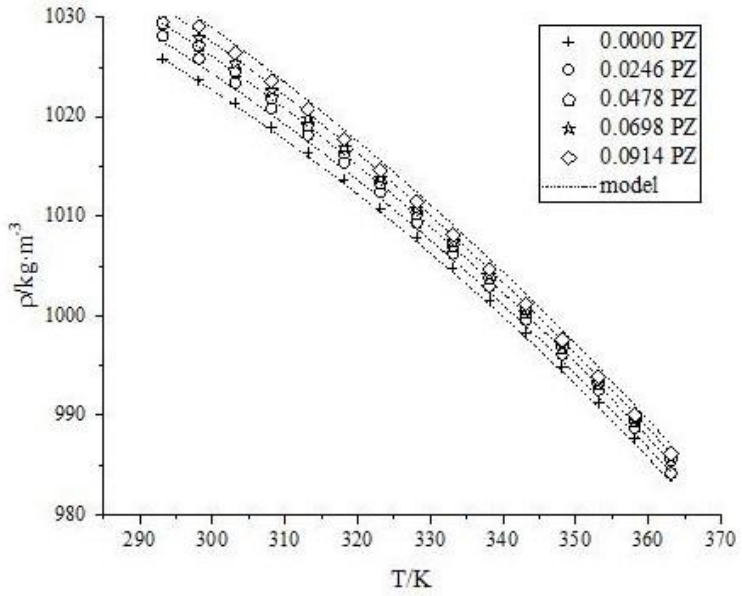
0.0000 PZ
0.0246 PZ
0.0478 PZ
0.0698 PZ
0.0914 PZ
model
ρ/kg·m-3
T/K

(a)

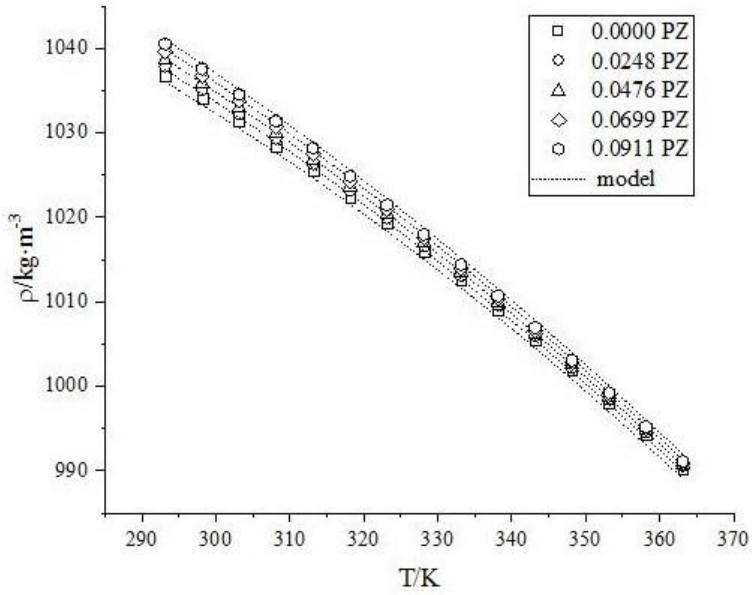
0.0000 PZ
0.0248 PZ
0.0476 PZ
0.0699 PZ
0.0911 PZ
model
ρ/kg·m-3
T/K

(b)

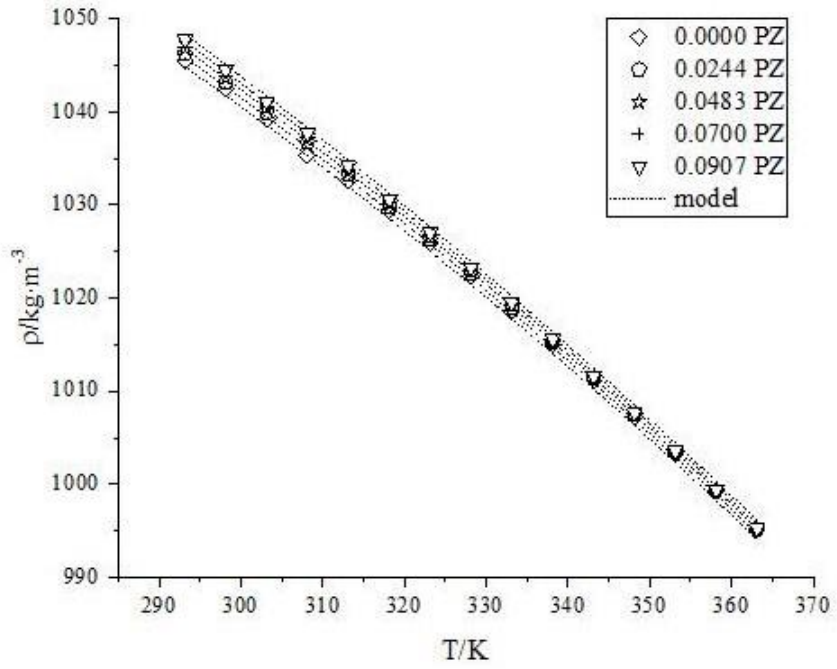

(c)

Figure 4.8: Densities of MDEA (1) + PZ (2) + H_2O (3) solutions as a function of temperature for the mass fractions of PZ in constant (a) 30/70 (b) 40/60 (c) 50/50 MDEA/H_2O solution. Symbols denote experimental data and dotted lines are calculated by the model, equation (4-11).

In addition, a spread in (shrinkage) behavior can be observed as the curves move towards downstream of the plots in Figure 4.8 (a), (b) and (c). This behavior could suggests that the density values of each of the ternary system are converging to a common value as the temperature increases. To provide a better insight of what is happening scientifically in the region of very high temperatures (above 363K), it is recommended (as further work) that the density measurement of MDEA + PZ +H_2O should be studied at very high temperatures (above 363.15K).

5 Conclusion

New experimental data for the densities of MEA (1) + 3DMA1P (2) + H_2O (3) ternary aqueous solution and its constituent MEA (1) + 3DMA1P (2) binary mixture have been presented and studied in the temperature range (298.15 to 353.15) K and atmospheric pressure, for 0.3 and 0.5 total amine mass fractions for the aqueous ternary system (MEA (1) + 3DMA1P (2) + H_2O (3)), as well as the whole composition range of the binary (MEA (1) + 3DMA1P (2)) system. The density data were correlated with temperature using linear equations with fitted parameters. The average absolute deviations and standard deviations were within the experimental uncertainties, which shows a satisfactory agreement between the measured and correlated data.

To represent deviations from ideal mixtures, excess molar volumes were calculated from the density data, and correlated using Redlich-Kister equation for binary mixtures and Nagata-Tamura equation for the ternary solutions. The minimal standard deviations indicates that the correlation is good. Radojkovic et al., Kohler and Jacob-Fitzer models were employed to predict the excess molar volumes of the ternary aqueous solutions and the best agreement was achieved by the Radojkovic et al. model, and as such, it is the best to use in the absence of ternary data.

Another new experimental density data of MDEA (1) + PZ (2) + H_2O (3) ternary amine solution in the temperature range of (293.15 to 363.15) K, and atmospheric pressure were produced. The PZ mass fraction was varied between 0 to 0.1 in each of the constant MDEA/H_2O binary solution of 0.3/0.7, 0.4/0.6 and 0.5/0.5. All the densities were correlated with a single polynomial equation yielding a slight standard deviation of 0.0094 kg/m^3 which is within the combined expanded uncertainty (0.414 kg/m^3), and a R^2 value of 1. This concludes that there is excellent agreement between the experimental and the correlated data.

6 Further work

The further work can be approached in two perspectives; the big one and the relatively small one. As a big approach from the context of the ultimate aim of this research which is to utilize this data in CO_2 absorption and desorption processes and other engineering applications. It is recommended as further work that other different amine solution densities should be measured and studied, particularly those ones that little or no attention has been given to.

The relatively small one which is closely related to this research work, is highlighted -in order of priority owing to my literature findings -as follows:

- Experimental density data should be produced and analyzed for both MEA + 3DMA1P + H_2O and MDEA + PZ + H_2O amine CO_2 loaded solutions -at various temperatures- which will become quaternary amine solutions. Although, the study will be more laborious due to the increase in number of components.
- A ThermoData engine (TDA) which was the first full scale software implementation algorithm, developed by [25] that is used in evaluating thermophysical properties of ternary chemical systems should be used for the ternary systems in this research work. In addition to this, the Prigogine-Flory-Patterson theory which is widely used to establish excess thermodynamic properties from binary constituents [47], should be used to predict the excess molar volumes reported in this work. To my best knowledge, very few or no information of these models have been used for amine solutions.
- Densities at high temperatures (above 363.15 K) should be measured for the CO_2 loaded and unloaded MEA + 3DMA1P + H_2O and MDEA + PZ + H_2O amine solutions. This work will have a very good application in the regeneration of CO_2 because regeneration is usually done at very high temperatures. It will also be useful in having better insight of what happens to the densities of MDEA + PZ + H_2O amine solutions at high temperatures as explained in Chapter 4.2.
- Available different models can be used to correlate the measured density data in this work, and the correlated data is compared with the measured data in line with experimental uncertainties.

References

[1] Wikipedia. (2016, 12-April). *History of climate change science --- Wikipedia{,} The Free Encyclopedia*. Available: https://en.wikipedia.org/w/index.php?title=History_of_climate_change_science&oldid=709120795

[2] C. K. Foo, C. Y. Leo, R. Aramesh, M. K. Aroua, N. Aghamohammadi, M. S. Shafeeyan, *et al.*, "Density and viscosity of aqueous mixtures of N-methyldiethanolamines (MDEA), piperazine (PZ) and ionic liquids," *Journal of Molecular Liquids,* vol. 209, pp. 596-602, 9// 2015.

[3] H. Arcis, Y. Coulier, K. Ballerat-Busserolles, L. Rodier, and J.-Y. Coxam, "Enthalpy of Solution of CO2 in Aqueous Solutions of Primary Alkanolamines: A Comparative Study of Hindered and Nonhindered Amine-Based Solvents," *Industrial & Engineering Chemistry Research,* vol. 53, pp. 10876-10885, 2014/07/09 2014.

[4] D. Fu, L. Qin, and H. Hao, "Experiment and model for the viscosity of carbonated piperazine-N-methyldiethanolamine aqueous solutions," *Journal of Molecular Liquids,* vol. 186, pp. 81-84, 10// 2013.

[5] S. Paul and B. Mandal, "Density and Viscosity of Aqueous Solutions of (N-Methyldiethanolamine + Piperazine) and (2-Amino-2-methyl-1-propanol + Piperazine) from (288 to 333) K," *Journal of Chemical & Engineering Data,* vol. 51, pp. 1808-1810, 2006/09/01 2006.

[6] O. Redlich and A. T. Kister, "Algebraic Representation of Thermodynamic Properties and the Classification of Solutions," *Industrial & Engineering Chemistry,* vol. 40, pp. 345-348, 1948/02/01 1948.

[7] X. Xu, C. Zhu, and Y. Ma, "Densities and Viscosities of Sugar Alcohols in Vitamin B6 Aqueous Solutions at (293.15 to 323.15) K," *Journal of Chemical & Engineering Data,* vol. 60, pp. 1535-1543, 2015/06/11 2015.

[8] P. Sipos, A. Stanley, S. Bevis, G. Hefter, and P. M. May, "Viscosities and Densities of Concentrated Aqueous NaOH/NaAl(OH)4 Mixtures at 25 °C," *Journal of Chemical & Engineering Data,* vol. 46, pp. 657-661, 2001/05/01 2001.

[9] R. H. Weiland, J. C. Dingman, D. B. Cronin, and G. J. Browning, "Density and Viscosity of Some Partially Carbonated Aqueous Alkanolamine Solutions and Their Blends," *Journal of Chemical & Engineering Data,* vol. 43, pp. 378-382, 1998/05/01 1998.

[10] J. M. Smith, H. C. Van Ness, and M. M. Abbott, *Introduction to chemical engineering thermodynamics*. Boston: McGraw-Hill, 2005.

[11] H. Zarei and Z. Salami, "Densities, Excess Molar Volumes, Viscosity, and Refractive Indices of Binary Mixtures of Ethanoic Acid and Trichloroethylene with Dimethylbenzenes at Different Temperatures," *Journal of Chemical & Engineering Data,* vol. 57, pp. 620-625, 2012/02/09 2012.

[12] N. A. Ghani, N. A. Sairi, M. K. Aroua, Y. Alias, and R. Yusoff, "Density, Surface Tension, and Viscosity of Ionic Liquids (1-Ethyl-3-methylimidazolium diethylphosphate and 1,3-Dimethylimidazolium dimethylphosphate) Aqueous Ternary Mixtures with MDEA," *Journal of Chemical & Engineering Data,* vol. 59, pp. 1737-1746, 2014/06/12 2014.

[13] A. V. Rayer and A. Henni, "Heats of Absorption of CO2 in Aqueous Solutions of Tertiary Amines: N-Methyldiethanolamine, 3-Dimethylamino-1-propanol, and 1-Dimethylamino-2-propanol," *Industrial & Engineering Chemistry Research,* vol. 53, pp. 4953-4965, 2014/03/26 2014.

[14] D. Ginsburg and R. Robinson, *Concerning Amines: Their Properties, Preparation and Reactions*: Elsevier Science, 2014.

[15] C. H. Hsu, H. Chu, and C. M. Cho, "Absorption and Reaction Kinetics of Amines and Ammonia Solutions with Carbon Dioxide in Flue Gas," *Journal of the Air & Waste Management Association,* vol. 53, pp. 246-252, 2003/02/01 2003.

[16] A. Veawab, P. Tontiwachwuthikul, and A. Chakma, "Influence of Process Parameters on Corrosion Behavior in a Sterically Hindered Amine−CO2 System," *Industrial & Engineering Chemistry Research,* vol. 38, pp. 310-315, 1999/01/01 1999.

[17] E. Pistikopoulos, M. Georgiadis, and V. Dua, *Process Systems Engineering: Volume 6: Molecular Systems Engineering*: John Wiley & Sons, 2010.

[18] R. F. Boehm, *Developments in the Design of Thermal Systems*: Cambridge University Press, 2005.

[19] J. Zhang, P. S. Fennell, and J. P. M. Trusler, "Density and Viscosity of Partially Carbonated Aqueous Tertiary Alkanolamine Solutions at Temperatures between (298.15 and 353.15) K," *Journal of Chemical & Engineering Data,* vol. 60, pp. 2392-2399, 2015/08/13 2015.

[20] J. Han, J. Jin, D. A. Eimer, and M. C. Melaaen, "Density of Water (1) + Diethanolamine (2) + CO2 (3) and Water (1) + N-Methyldiethanolamine (2) + CO2 (3) from (298.15 to 423.15) K," *Journal of Chemical & Engineering Data,* vol. 57, pp. 1843-1850, 2012/06/14 2012.

[21] J. Han, J. Jin, D. A. Eimer, and M. C. Melaaen, "Density of Water (1) + Monoethanolamine (2) + CO2 (3) from (298.15 to 413.15) K and Surface Tension of Water (1) + Monoethanolamine (2) from (303.15 to 333.15) K," *Journal of Chemical & Engineering Data,* vol. 57, pp. 1095-1103, 2012/04/12 2012.

[22] X. Wang, J. Chen, and X. Wang, "Densities and excess molar volumes of the binary system N-methyldiethanolamine + (2-aminoethyl)ethanolamine and its ternary aqueous mixtures from 283.15 to 363.15 K," *Physics and Chemistry of Liquids,* vol. 54, pp. 499-506, 2016/07/03 2016.

[23] Z. Idris, J. Chen, and D. A. Eimer, "Densities of unloaded and CO2-loaded 3-dimethylamino-1-propanol at temperatures (293.15 to 343.15) K," *The Journal of Chemical Thermodynamics,* vol. 97, pp. 282-289, 6// 2016.

[24] P. W. J. Derks, E. S. Hamborg, J. A. Hogendoorn, J. P. M. Niederer, and G. F. Versteeg, "Densities, Viscosities, and Liquid Diffusivities in Aqueous Piperazine and Aqueous (Piperazine + N-Methyldiethanolamine) Solutions," *Journal of Chemical & Engineering Data,* vol. 53, pp. 1179-1185, 2008/05/01 2008.

[25] V. Diky, R. D. Chirico, C. D. Muzny, A. F. Kazakov, K. Kroenlein, J. W. Magee, *et al.*, "ThermoData Engine (TDE) Software Implementation of the Dynamic Data Evaluation Concept. 7. Ternary Mixtures," *Journal of Chemical Information and Modeling,* vol. 52, pp. 260-276, 2012/01/23 2012.

[26] Z. Idris, L. Ang, D. A. Eimer, and J. Ying, "Density Measurements of Unloaded and CO2-Loaded 1-Dimethylamino-2-propanol at Temperatures (298.15 to 353.15) K," *Journal of Chemical & Engineering Data,* vol. 60, pp. 1419-1425, 2015/05/14 2015.

[27] F. Spieweck and H. Bettin, "Solid and liquid density determination " *Technisches Messen* vol. 59, pp. 285-292, 1992.

[28] G. L. Squires, *Practical Physics*: Cambridge University Press, 2001.

[29] L. Kirkup and R. B. Frenkel, *An Introduction to Uncertainty in Measurement: Using the GUM (Guide to the Expression of Uncertainty in Measurement)*: Cambridge University Press, 2006.

[30] W. B. Whiting, "Effects of Uncertainties in Thermodynamic Data and Models on Process Calculations," *Journal of Chemical & Engineering Data,* vol. 41, pp. 935-941, 1996/01/01 1996.

[31] P. De Bièvre and H. Günzler, *Measurement Uncertainty in Chemical Analysis*: Springer Berlin Heidelberg, 2013.

[32] E. S. Menon, *Liquid Pipeline Hydraulics*: CRC Press, 2004.

[33] A. Blanco, A. García-Abuín, D. Gómez-Díaz, and J. M. Navaza, "Density, Speed of Sound, Viscosity, and Surface Tension of Dimethylethylenediamine + Water and (Ethanolamine + Dimethylethanolamine) + Water from T = (293.15 to 323.15) K," *Journal of Chemical & Engineering Data,* vol. 61, pp. 188-194, 2016/01/14 2016.

[34] P. R. Bevington and D. K. Robinson, *Data Reduction and Error Analysis for the Physical Sciences*: McGraw-Hill, 2003.

[35] A. R. Mahajan and S. R. Mirgane, "Excess Molar Volumes and Viscosities for the Binary Mixtures of n-Octane, n-Decane, n-Dodecane, and n-Tetradecane with Octan-2-ol at 298.15 K," *Journal of Thermodynamics,* vol. 2013, p. 11, 2013.

[36] J. D. Smiljanić, M. L. Kijevčanin, B. D. Djordjević, D. K. Grozdanić, and S. P. Šerbanović, "Temperature Dependence of Densities and Excess Molar Volumes of the Ternary Mixture (1-Butanol + Chloroform + Benzene) and its Binary Constituents (1-Butanol + Chloroform and 1-Butanol + Benzene)," *International Journal of Thermophysics,* vol. 29, pp. 586-609, 2008.

[37] A. M. Awwad, "Densities and Excess Molar Volumes of N-Methylmorpholine + 1-Alkanol Systems at 298.15 K," *Journal of Chemical & Engineering Data,* vol. 53, pp. 307-309, 2008/01/01 2008.

[38] F. Comelli and R. Francesconi, "Excess Molar Enthalpies and Excess Molar Volumes of Propionic Acid + Octane, + Cyclohexane, + 1,3,5-Trimethylbenzene, + Oxane, or + 1,4-Dioxane at 313.15 K," *Journal of Chemical & Engineering Data,* vol. 41, pp. 101-104, 1996/01/01 1996.

[39] N. Deenadayalu and P. Bhujrajh, "Density, Speed of Sound, and Derived Thermodynamic Properties of Ionic Liquids [EMIM]+[BETI]− or ([EMIM]+[CH3(OCH2CH2)2OSO3]− + Methanol or + Acetone) at T = (298.15 or 303.15 or 313.15) K," *Journal of Chemical & Engineering Data,* vol. 53, pp. 1098-1102, 2008/05/01 2008.

[40] N. Deenadayalu, I. Bahadur, and T. Hofman, "Ternary Excess Molar Volumes of {Methyltrioctylammonium Bis[(trifluoromethyl)sulfonyl]imide + Methanol + Methyl Acetate or Ethyl Acetate} Systems at (298.15, 303.15, and 313.15) K," *Journal of Chemical & Engineering Data,* vol. 55, pp. 2636-2642, 2010/07/08 2010.

[41] N. Isamu and T. Kazuhiro, "Excess molar enthalpies of {methanol or ethanol + (2-butanone + benzene)} at 298.15 K," *The Journal of Chemical Thermodynamics,* vol. 22, pp. 279-283, 1990.

[42] A. Arce, E. Rodil, and A. Soto, "Property Changes of Mixing for the 1-Butanol + Methanol + 2-Methoxy-2-methylbutane System at 298.15 K and Atmospheric Pressure," *Journal of Chemical & Engineering Data,* vol. 46, pp. 962-966, 2001/07/01 2001.

[43] N. Radojković, A. Tasić, D. Grozdanić, B. Djordjević, and D. Malić, "Excess volumes of acetone + benzene, acetone + cyclohexane, and acetone + benzene + cyclohexane at 298.15 K," *The Journal of Chemical Thermodynamics,* vol. 9, pp. 349-356, 1977/04/01 1977.

[44] F. Kohler, "Estimation of the thermodynamic data for a ternary system from the corresponding binary systems," *Monatshefte fur Chemie,* vol. 91, pp. 738-740, 1960.

[45] K. T. Jacob and K. Fitzner, "The estimation of the thermodynamic properties of ternary alloys from binary data using the shortest distance composition path," *Thermochimica Acta,* vol. 18, pp. 197-206, 1977/02/01 1977.

[46] A. Samanta and S. S. Bandyopadhyay, "Density and Viscosity of Aqueous Solutions of Piperazine and (2-Amino-2-methyl-1-propanol + Piperazine) from 298 to 333 K," *Journal of Chemical & Engineering Data,* vol. 51, pp. 467-470, 2006/03/01 2006.

[47] A. C. Galvão and A. Z. Francesconi, "Application of the Prigogine–Flory–Patterson model to excess molar enthalpy of binary liquid mixtures containing acetonitrile and 1-alkanol," *Journal of Molecular Liquids,* vol. 139, pp. 110-116, 3/15/ 2008.

Appendices

Appendix A: Task Description

Appendix B: Rotary Vapor Details

Appendix C: Density measurement procedure

Appendix D: Predictive Models of Ternary Data

Appendix E: Densities of MDEA + PZ +H_2O ternary data

Appendix A: Task description

Telemark University College
Faculty of Technology

FMH606 Master's Thesis

Title: Measurement and correlation of data used for CO_2 absorption in different amine solutions at various temperatures.

TUC supervisors: Professor Dag Eimer, assisted by Dr Zulkifli Idris

External partner: Tel-Tek

Task description:

The task is to measure densities of aqueous amine solutions, with and without CO_2, to various levels at a range of temperatures. The data shall be correlated by fitting parameters to appropriate models such that these models can account for mixture densities at various temperatures, amine concentrations and CO_2 loadings. Literature review is of course part of this work. The amines to focus on are identified, but will be chosen to fit into an ongoing research project.

All data measured shall be analyzed and correlated. Uncertainties shall be estimated. Formal chemical engineering analysis shall be applied to all details of the method.

Final thesis shall include literature review, review and description of experimental technique, theoretical treatment and a discussion of the work and achievements. It should also be noted that reliable and producible results from this work will be submitted to a peer-reviewed international journal, and the student will be one of the co-authors.

Task background:

Carbon dioxide (CO_2) is considered as one of the main contributors to the global warming and the removal of CO_2 from industrial gas streams has become even more important due to the focus on reduction of greenhouse gas emissions.

Amine based chemical absorption processes is the main method for removal of CO_2. MEA has been employed as an important industrial absorbent with its rapid reaction rate,

Address: Kjølnes ring 56, NO-3918 Porsgrunn, Norway. **Phone:** 35 57 50 00. **Fax:** 35 55 75 47.

relative low cost and thermal stability. However, other amines are being considered in an attempt to lower capture costs.

This work is an integral and important part of a big research effort financed the Norwegian Research Council. The focus of this project is to develop predictive equilibrium models.

Physical data including solution densities are important parameters for industrial design estimates. There is still uncharted territory.

Student category:

PT or EET students

Practical arrangements:
Laboratory facilities will be provided and is ready to use.

Signatures:

Student (date and signature):

Supervisors (date and signature):

Appendix B: Details of Rotary Vapor

6 Operation

This chapter explains the operating elements and possible operating modes. It gives instructions on how to operate the instrument properly and safely.

ATTENTION

Check the glassware for damages prior to each operation and use only glassware in perfect condition. Glassware with cracks, stars or other damages can break during operation.

6.1 Starting the pump

6.1.1 Pump without controller

After the pump is completely installed it is ready to operate, i.e. when the mains switch is pressed, the pump starts operating right away and starts evacuating until the end vacuum (10 mbar with the V-700 and 2 mbar with the V-710). When the pump is operated continuously over a longer period of time it automatically switches to the ECO² Mode (see chapter 4.5). In case the Vacuum Pump V-700 or V-710 is part of a central lab source pump we recommend to use the Vacuum Module V-802 LabVac to ensure an unreduced suction power during the whole operation time (see chapter 4.4).

6.1.2 Pump with controller

After the pump and the controller are completely installed, the system is ready to operate. When the mains switch is pressed, the pump is on standby and starts operating as soon as the controller is started. It then evacuates to the vacuum preset at the controller.

6.1.3 EasyVac

For a description of the EasyVac function, see chapter 4.3.

6.1.4 LabVac

For a description of the LabVac function, see chapter 4.4.

6.1.5 ECO² Mode

For a description of the ECO² Mode, see chapter 4.5.

6.2 Selecting the distillation conditions

To achieve optimal distillation conditions, the distillation energy supplied by the heating bath must be removed by the condenser.

To ensure this, operate the instrument according to the following rule of thumb:

Cooling water: max. 20 °C **Vapor: 40 °C** **Bath: 60 °C**

How are these conditions achieved?:

- Set the bath temperature to 60 °C.
- Set the cooling water temperature not higher than 20 °C.
- Allow cooling water to flow through the condenser at approximately 40 – 50 l/h.
- Define the operating vacuum in such a way, that the boiling point of the solvent is 40 °C. The corresponding pressure can be seen from the Solvent Table in chapter 3.

Advantages associated with bath temperatures of 60 °C:

- The evaporating flask can be replaced without risk of burns.
- The evaporation rate of the water from the heating bath is low (low energy loss).
- The heating bath energy is used at a good degree of efficiency.

This rule can also be applied to lower bath temperatures, e.g.:

Cooling water: 0 °C **Vapor: 20 °C** **Bath: 40 °C**

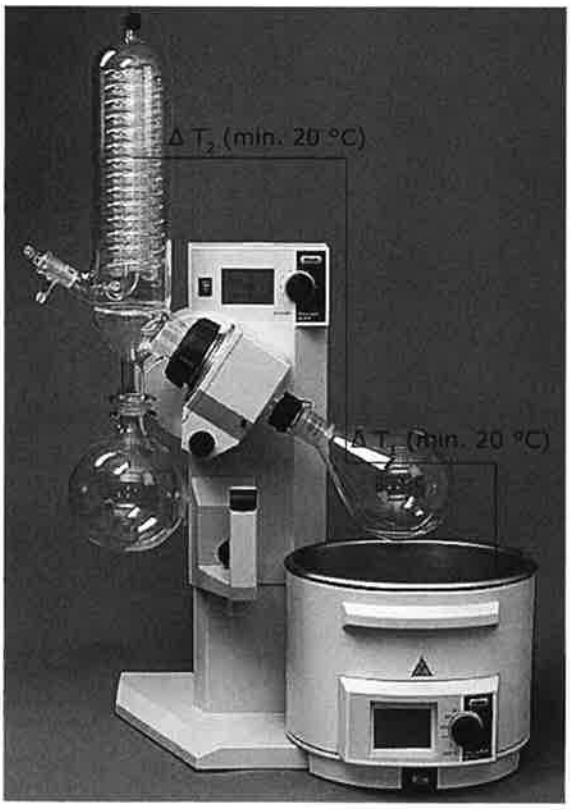

Fig. 6.1: 20-40-60 ° rule

6.3 Optimizing the distillation conditions

Depending on the solvent being distilled the distillation might have to be re-optimized. In the optimized case, the condenser should be steamed up to between 2/3 to 3/4, see figure below.

If this is not the case, there are two possibilities to optimize the distillation:

- When the heating bath has reached 60 °C slowly reduce the pressure. Thus, the boiling point of the solvent is reduced and ΔT_1 increases resulting in an increase of distillation capacity.
- When the heating bath has reached 60 °C increase the bath temperature. Thus ΔT_1 increases resulting in an increase of distillation capacity as well.

NOTE

When the bath temperature is increased, not all of the additional energy is used for distillation but a major part is discharged into the environment due to the increasing difference between heating bath and the ambient temperature.

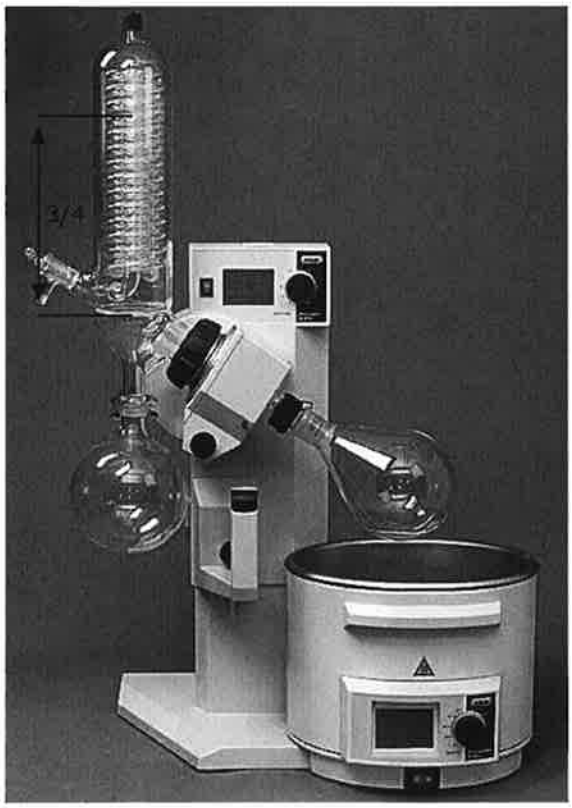

Fig. 6.2: Optional condensation area of a condenser

Appendix C: Density meter Procedures

Hints:

- After turning on the power, the DMA needs approx. 20 minutes for attemperating and additionally 5 to 10 minutes for internal temperature adjustments. During this time "attemperating" is displayed. If the desired measuring temperature is already set, do not touch any key during this time as this will considerably increase the waiting period.
- In case of high air humidity or low measuring temperatures see Appendix A.

14. As soon as the attemperating of the DMA to 20 °C is finished, perform a density check measurement using the supplied liquid density standards (see Chapter 7.2).

Important:
The DMA is factory adjusted and this control measurement should be performed to check if the adjustment is still valid after transport.

6 General Settings

6.1 Menu Operation

Hint:
For a graphic overview, see the menu tree in Appendix F.

Using the Keys on the Keypad

- To select the main menu press the "Menu" soft key.
- To select menu items use the "UP" or "DOWN" keys and press "↵" to confirm the selection.
- In the submenus found under "method settings", "output selection" and "memory configuration" and "printer configuration" toggle between "Y" (yes, selected) and "N" (no, not selected) using the "↵" key. Move to the next item using the "UP" and "DOWN" keys.
- In the submenus found under "method settings", "display configuration" toggle between "N" (no, not selected), "S" (small size), "M" (medium size) and "L" (large size) using the "↵" key.
- In the other submenus, to select a menu item
  - press "↵" to activate the item,
  - move the cursor to the desired position using the "Left" or "Right" soft keys,

- decrease or increase the numerical value of a digit by using the "UP" or "DOWN" keys,
- select letters and numbers by using the "UP" or "DOWN" keys,
- conclude the setting by pressing "↵".

- To return to the previous display press the "Esc" soft key.
- To save changed data press the "Yes" soft key upon the question "Save changes?".
- To return to the measuring mode press the "Exit" soft key.

6.2 Display Contrast

- Make sure that the instrument is set to the measuring mode.
- The display contrast is adjusted by pressing the "UP" or "DOWN" keys.
- Save the setting of the display contrast permanently in the "instrument settings", "save display contrast" menu.

6.3 Setting Date and Time

Date and time are set in the "instrument settings", "date & time" menu. Different formats can be selected.

6.4 Setting the Language

Select the language (English or German) in the menu "instrument settings", "language".

6.5 Defining a Method

- A method consists of the following settings: measuring temperature, display settings, printer and memory configuration, measurement settings and control settings for the optional sample changer. These are all stored under a unique method name. 10 different methods can be assigned.
- The 10 methods are factory preset, covering the most common measuring tasks. However, every method can be individually changed, adapted or renamed.
- To activate a method, press the "Method" soft key and select a method from the list by pressing "↵".
- To rename the method select "method settings", "edit method name".

- The factory setting for each method can be recalled by selecting "reset method" in the menu "method settings".

6.6 Setting the Temperature

Set the temperature to degrees Celsius (°C) or Fahrenheit (°F) in "temperature setting".

6.7 Settings for the Measuring Procedure

The parameters for the measuring procedure are set in "measurement settings".

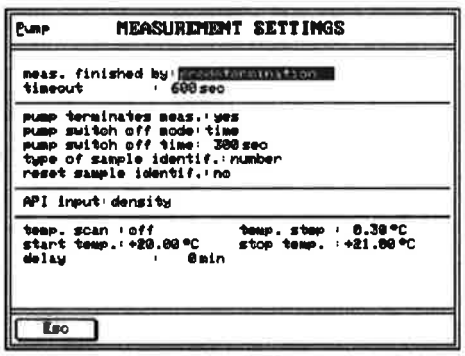

Fig. 6 - 1 DMA 5000 screen: Measurement settings

For the fastest results (approx. 1 minute), set the parameter "meas. finished by: predetermination". The DMA calculates the density before complete temperature equilibrium has been reached.

For the highest accuracy results, set the parameter "meas. finished by: equilibrium". The DMA determines the density and concentration after complete temperature equilibrium has been reached.

In the **DMA 5000** for higher accuracy 3 methods can be selected: Equilibrium fast, Equilibrium medium, Equilibrium slow. The highest accuracy is achieved by using Equilibrium slow.

- "pump terminates measurement": If "yes" is selected, activating the air pump will interrupt the measurement.
- "pump switch off mode": If "time" is selected the air pump will be switched off automatically after the specified "pump switch off time". Otherwise the air pump has to be switched off manually.
- Select the type of sample identification in "type of sample identif.".

- "reset sample identif.": Select if the entered sample identification should be deleted after the measurement.
- "API input": Select the kind of density for calculating the API functions: density, density (not viscosity correct.), special adjustment 0-4.

DMA 5000:

- "delay": This function is only available when a temperature scan is activated. When measurements are carried out with the temperature scan, a "delay time" (from 0 to 9999 minutes) can be entered: After reaching the new measuring temperature, the DMA 5000 waits for the set time before the measurement is carried out.
- "temp. scan": Measurements by different temperatures are performed automatically. Start, end and step values can be entered.

7 Checking Procedure, Adjustment and Calibration

7.1 Definitions

Adjustment of the density meter:

- The process of bringing the instrument into a state suitable for use, by setting or adjusting the density instrument constants.

Calibration of the density meter:

- Various processes for establishing the relationship between the reference density of measurement standards and the corresponding density reading of the instrument.
- Calibrations are performed to determine the deviation of the displayed density values from the reference values of density standards.

7.2 Checking Procedure: Density Check

The "density check" function allows you either to check the validity of the factory adjustment after transport or the validity of your own adjustments.

- To check the factory adjustment, pure water is used as calibration fluid.
- To check your own adjustments either degassed, bi-distilled water or different density calibration fluids or standardized samples can be used.

- Before each series of measurements check the validity of the adjustment using degassed, bi-distilled water or an appropriate density standard.
- The density check should be performed once every day.

Hint:
Preparation of degassed, bi-distilled water:
1. Boil fresh, bi-distilled water for several minutes to remove dissolved air.
2. Fill a clean glass flask full with the boiled water and cover it.
3. Wait until the water has cooled down to the approx. measuring temperature.

Performing the density check:

1. Select "adjustment", "density check", "density check settings".
2. Enter the settings corresponding to the density calibration fluid.

Hint:
For water the following settings are recommended:
density: 0.99820 (DMA 4100/4500); 0.998203 (DMA 5000)
max. dens. dev.: 0.00010 g/cm^3 (DMA 4100/4500);
0.00005 g/cm^3 (DMA 5000)
temperature: +20.00 °C
check interval: 1 day
check density: on
Switching on "check density" activates a memory function. If the interval (1-999 days) is expired, a flashing "Density Check Needed" in the headline of the measuring window will appear.

3. Select "check density" to start the density check (the corresponding steps are shown on the display).
4. - If the measured density is within the permitted range, the display shows "density check: OK". Routine measurements can be carried out.
   - If the measured density is out of range, the display shows "density check: NOT OK". Clean and dry the measuring cell and repeat the density check. If the result is still "density check: NOT OK", perform a new adjustment (see Chapter 7.3).

Hint:
In each case ("density check: OK" or "density check: NOT OK") the measured density and the deviation from the set density are displayed.

5. Up to 50 density checks can be stored with date and time. The activated density check or all stored density checks can be printed out.

7.3 Adjustment

- An adjustment has to be performed if deviations between the displayed values and reference values of density standards exceed the specifications of the DMA or the specifications of the standard.
- Air and bi-distilled, freshly degassed water are used for normal adjustment.
- A factory setting allows density measurements over the entire temperature range, although adjustment is usually only performed at 20 °C.
- If measurements at different temperatures indicate deviations between the displayed values on the DMA and reference values of density standards, then an air and water adjustment for the whole temperature range is necessary (see Chapter 7.3.2).

Hint:
It is not recommended and does not improve the performance of the DMA to adjust if calibrations with suitable density standards indicate no deviations from the reference values.

7.3.1 Adjustment with Air and Water at 20 °C

Normal adjustment (5-10 min) is performed using dry air (see Appendix A) and bi-distilled, freshly degassed water at 20 °C.

Adjustment procedure at 20 °C:

1. Before adjustment thoroughly clean and dry the measuring cell (see Chapter 9).
2. Press the "Menu" key and select the menus "adjustment", "adjust" and "density (air, water)" using the "UP", "DOWN" and "↵" keys.

Hint:
If the DMA is set to any other temperature, it will automatically be switched to 20 °C when the adjustment procedure is started.

3. Start the adjustment by pressing the "OK" key.
4. Press the "↵" key and enter the current air pressure using the "UP", "DOWN", "Left", "Right" and "↵" keys.

Hints:

- For air adjustment, the current air pressure must be entered, as it influences the air density.
- The density values of water and air at a specific atmospheric pressure for the complete temperature range are stored in the memory.
- If the current on-site barometric pressure is not available, enter the average air pressure (depending on the altitude above sea level) according to the following table:

Table 7.1: Altitude and air pressure

Altitude above sea level		Air pressure
[m]	[ft]	[mbar]
0	0	1013
400	1312	966
800	2625	921
1200	3937	877
1600	5249	835
2000	6562	795
2400	7874	756
2800	9186	719
3200	10499	683
3600	11811	649

5. Wait until the air adjustment is finished.

6. Fill the measuring cell with bi-distilled, freshly degassed water, checking for the presence of bubbles through the viewing window.

Hint:
For the degassing of water, see Chapter 7.2.

7. Start the water adjustment by pressing the "OK" key.

8. Wait until the water adjustment is finished. After pressing the "OK" key the deviation of the new adjustment from the last adjustment performed is displayed at a density of 1 g/cm^3.

9. • The adjustment is saved by selecting "SAVE" after "recommendation: SAVE" is displayed. The adjustment data are stored and can be printed if a printer is connected and activated.
   • By selecting "REPEAT" after "recommendation: REPEAT" is displayed, the adjustment is repeated (if the deviation is ≥ 0.00005 g/cm^3). Clean the measuring cell first (Chapter 9). If the deviation remains unchanged, the adjustment can be stored by selecting "SAVE".

7.3.2 Adjustment with Air and Water for the Entire Temperature Range (Full Range Adjustment)

If measurements at different temperatures indicate deviations between the displayed values on the DMA and reference values of density standards, then an air and water adjustment for the whole temperature range (2 hours) is necessary. Dry air (Appendix A) and bi-distilled, freshly degassed water are used.

The adjustment procedure is performed as follows:

- Air adjustment at 40 °C
- Air adjustment at 60 °C
- Water adjustment at 40 °C
- Water adjustment at 60 °C

Full range adjustment procedure:

1. Perform an air and water adjustment at 20 °C (see Chapter 7.3.1).
2. Thoroughly clean and dry the measuring cell (see Chapter 9).
3. Press the "Menu" key and select the menus "adjustment", "adjust" and "density (temperature range)" using the "UP", "DOWN" and "↵" keys.
4. Start the full range adjustment by pressing the "OK" key.
5. Perform all further steps as is required by the instrument.

Hint:
Bi-distilled water is degassed by boiling it, cooled to 65 to 60 °C and filled bubble-free into the measuring cell using a syringe.

6. For saving the adjustment proceed as described in Chapter 7.3.1.

7.3.3 Special Adjustment

Special adjustment (user-specific adjustments) should only be performed if e.g. a norm explicitly demands an adjustment different from the above-mentioned adjustment. During special adjustments no correction of the viscosity will be performed (see reference manual chapter 8.3.3).

7.4 Calibration

- Calibrations are carried out using certified liquid density standards.
- The displayed density value on the DMA is compared to the reference value indicated in the calibration certificate of the liquid density standard.
- The physical properties (density, viscosity) of the liquid density standards should be similar to those of the samples.

- The frequency of calibrations with certified liquid density standards depends on the requirements and the user's judgement. Recommendation: 1 to 2 calibrations per year.

- Notes on the 5 liquid density standards, supplied with the DMA:

  - The density of the ultra pure water (density standard) is given at different temperatures with an uncertainty of 0.00001 g/cm^3 at a confidence level of 95%.
  - The listed densities are valid for the time at which the liquids were filled.
  - The calibration liquids should be stored in a cool and dark place!
  - The calibration liquids must be used immediately and only once after the bottle has been opened!

Calibration procedure:

1. Perform a density check (see Chapter 7.2) with water and carry out an adjustment at 20 °C (see Chapter 7.3.1), if necessary.

2. Thoroughly clean and dry the measuring cell (see Chapter 9).

3. Immediately after opening the bottle, inject the liquid density standard by means of a glass or metal syringe without any air bubbles into the measuring cell of the DMA.

4. After the measurement is finished, print the result (density at given temperature).

5. Document the calibration procedure in a calibration protocol which contains the operator's name, date, place, description of the calibration procedure, results and the calibration certificate of the liquid density standard.

6. Perform a thorough cleaning of the measuring cell.

8 Measurements

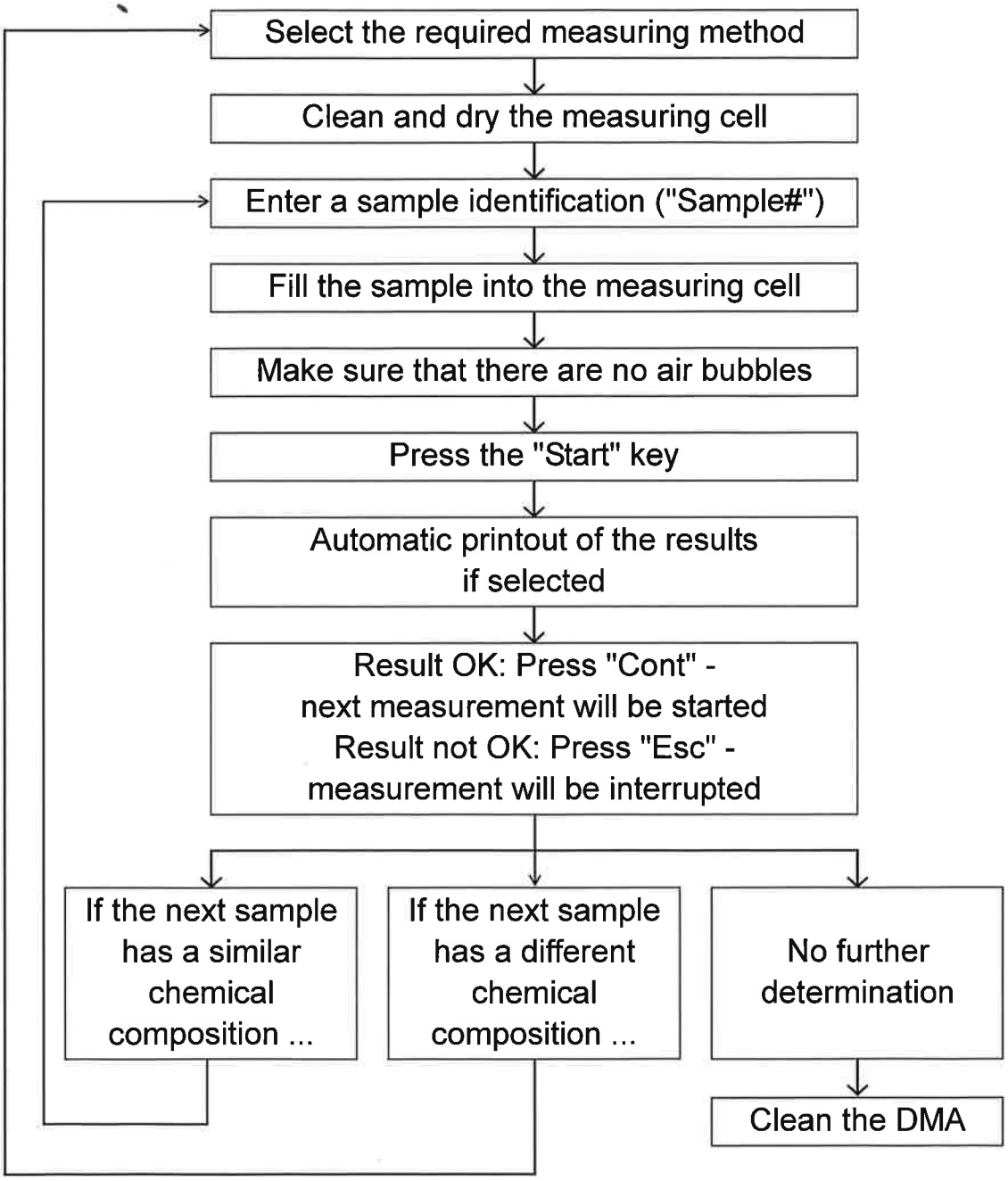

Appendix D:

Predicted models for excess molar volumes

Experimental And Radojkovic et al. Predicted Excess Molar Volumes V_m^E of MEA(1) + 3DMA1P(2) + H_2O(3) Ternary Systems at Different Temperatures (T), Mass (w), Mole (x) fractions and Atmospheric Pressure.

.

T	$V_m^E \cdot 10^{-6}$	Model	T	$V_m^E \cdot 10^{-6}$	Model
K	$m^3 \cdot mol^{-1}$	$m^3 \cdot mol^{-1}$	K	$m^3 \cdot mol^{-1}$	$m^3 \cdot mol^{-1}$
		$w_1 = 0.30$, $w_2 = 0$, $x_1 = 0.113$, $x_2 = 0$			
298.15	-0.2043	-0.1964	323.15	-0.1947	-0.1877
303.15	-0.2026	-0.1946	328.15	-0.1849	-0.1859
308.15	-0.2022	-0.1929	333.15	-0.1760	-0.1842
313.15	-0.2016	-0.1911	338.15	-0.1682	-0.1824
318.15	-0.1998	-0.1894	343.15	-0.1684	-0.1807
		$w_1 = 0.24$, $w_2 = 0.06$, $x_1 = 0.091$, $x_2 = 0.013$			
298.15	-0.2885	-0.2656	323.15	-0.2787	-0.2476
303.15	-0.2861	-0.2613	328.15	-0.2798	-0.2443
308.15	-0.2845	-0.2578	333.15	-0.2814	-0.2412
313.15	-0.2817	-0.2541	338.15	-0.2843	-0.2390
318.15	-0.2841	-0.2505	343.15	-0.2848	-0.2363
		$w_1 = 0.18$, $w_2 = 0.12$, $x_1 = 0.069$, $x_2 = 0.027$			
298.15	-0.3734	-0.3428	323.15	-0.3610	-0.3154
303.15	-0.3693	-0.3361	328.15	-0.3594	-0.3105
308.15	-0.3660	-0.3306	333.15	-0.3576	-0.3061
313.15	-0.3601	-0.3250	338.15	-0.3571	-0.3033
318.15	-0.3625	-0.3194	343.15	-0.3583	-0.2996
		$w_1 = 0.12$, $w_2 = 0.18$, $x_1 = 0.046$, $x_2 = 0.041$			
298.15	-0.4620	-0.4276	323.15	-0.4350	-0.3904
303.15	-0.4560	-0.4182	328.15	-0.3961	-0.3839
308.15	-0.4488	-0.4109	333.15	-0.4208	-0.3781
313.15	-0.4365	-0.4032	338.15	-0.4317	-0.3748
318.15	-0.4459	-0.3956	343.15	-0.4288	-0.3700
		$w_1 = 0.06$, $w_2 = 0.24$, $x_1 = 0.023$, $x_2 = 0.055$			
298.15	-0.5427	-0.5199	323.15	-0.5137	-0.4727
303.15	-0.5279	-0.5078	328.15	-0.5090	-0.4644
308.15	-0.5342	-0.4985	333.15	-0.5044	-0.4572
313.15	-0.5075	-0.4887	338.15	-0.4984	-0.4533

318.15	-0.5200	-0.4791	343.15	-0.4414	-0.4474
		$w_1 = 0$, $w_2 = 0.30$, $x_1 = 0$, $x_2 = 0.070$			
298.15	-0.6272	-0.6210	323.15	-0.5825	-0.5635
303.15	-0.6166	-0.6062	328.15	-0.5752	-0.5534
308.15	-0.6071	-0.5948	333.15	-0.5689	-0.5447
313.15	-0.5981	-0.5829	338.15	-0.5625	-0.5401
318.15	-0.5900	-0.5712	343.15	-0.5566	-0.5330
		$w_1 = 0.50$, $w_2 = 0$, $x_1 = 0.228$, $x_2 = 0$			
298.15	-0.4456	-0.4400	323.15	-0.4271	-0.4250
303.15	-0.4397	-0.4370	328.15	-0.4257	-0.4220
308.15	-0.4353	-0.4340	333.15	-0.4246	-0.4190
313.15	-0.4314	-0.4310	338.15	-0.4241	-0.4160
318.15	-0.4289	-0.4280	343.15	-0.4239	-0.4130
		$w_1 = 0.45$, $w_2 = 0.05$, $x_1 = 0.207$, $x_2 = 0.014$			
298.15	-0.5843	-0.4867	323.15	-0.5641	-0.4639
303.15	-0.5773	-0.4816	328.15	-0.5619	-0.4596
308.15	-0.5720	-0.4771	333.15	-0.5631	-0.4554
313.15	-0.5659	-0.4725	338.15	-0.5618	-0.4518
318.15	-0.5667	-0.4680	343.15	-0.5617	-0.4478
		$w_1 = 0.40$, $w_2 = 0.10$, $x_1 = 0.186$, $x_2 = 0.028$			
298.15	-0.6071	-0.5377	323.15	-0.5731	-0.5073
303.15	-0.5977	-0.5307	328.15	-0.5686	-0.5016
308.15	-0.5902	-0.5247	333.15	-0.5649	-0.4963
313.15	-0.5838	-0.5185	338.15	-0.5612	-0.4920
318.15	-0.5779	-0.5124	343.15	-0.5580	-0.4871
		$w_1 = 0.30$, $w_2 = 0.20$, $x_1 = 0.142$, $x_2 = 0.056$			
298.15	-0.7759	-0.6528	323.15	-0.7286	-0.6068
303.15	-0.7608	-0.6416	328.15	-0.7212	-0.5984
308.15	-0.7559	-0.6326	333.15	-0.7140	-0.5908
313.15	-0.7447	-0.6232	338.15	-0.7073	-0.5850
318.15	-0.7374	-0.6140	343.15	-0.7040	-0.5782
		$w_1 = 0.20$, $w_2 = 0.30$, $x_1 = 0.097$, $x_2 = 0.086$			
298.15	-0.9541	-0.7846	323.15	-0.8902	-0.7226
303.15	-0.9367	-0.7692	328.15	-0.8809	-0.7114
308.15	-0.9180	-0.7570	333.15	-0.8722	-0.7015
313.15	-0.9118	-0.7443	338.15	-0.8638	-0.6941
318.15	-0.9004	-0.7320	343.15	-0.8570	-0.6853
		$w_1 = 0.10$, $w_2 = 0.40$, $x_1 = 0.049$, $x_2 = 0.116$			
298.15	-1.0701	-0.9346	323.15	-0.9794	-0.8556
303.15	-1.0519	-0.9147	328.15	-0.9790	-0.8415
308.15	-1.0248	-0.8992	333.15	-0.9632	-0.8291
313.15	-1.0135	-0.8830	338.15	-0.9402	-0.8200
318.15	-1.0003	-0.8675	343.15	-0.9211	-0.8090

		$w_1 = 0.05$, $w_2 = 0.45$, $x_1 = 0.025$, $x_2 = 0.132$			
298.15	-1.1180	-1.0177	323.15	-1.0160	-0.9298
303.15	-1.0898	-0.9953	328.15	-0.9965	-0.9141
308.15	-1.0702	-0.9782	333.15	-0.9926	-0.9003
313.15	-1.0529	-0.9602	338.15	-0.9649	-0.8903
318.15	-1.0249	-0.9430	343.15	-0.9048	-0.8781
		$w_1 = 0$, $w_2 = 0.50$, $x_1 = 0$, $x_2 = 0.149$			
298.15	-1.1848	-1.1072	323.15	-1.0847	-1.0101
303.15	-1.1616	-1.0824	328.15	-1.0686	-0.9927
308.15	-1.1400	-1.0635	333.15	-1.0531	-0.9777
313.15	-1.1206	-1.0436	338.15	-1.0381	-0.9666
318.15	-1.1016	-1.0246	343.15	-1.0241	-0.9531

Experimental And Kohler-Predicted Excess Molar Volumes V_m^E of MEA(1) + 3DMA1P(2) + H_2O(3) Ternary Systems at Different Temperatures (T), Mass (w), Mole (x) fractions and Atmospheric Pressure.

T	**$V_m^E \cdot 10^{-6}$**	**Model**	**T**	**$V_m^E \cdot 10^{-6}$**	**Model**
K	**$m^3 \cdot mol^{-1}$**	**$m^3 \cdot mol^{-1}$**	**K**	**$m^3 \cdot mol^{-1}$**	**$m^3 \cdot mol^{-1}$**
		$w_1 = 0.30$, $w_2 = 0$, $x_1 = 0.113$, $x_2 = 0$			
298.15	-0.2043	-0.1964	323.15	-0.1947	-0.1877
303.15	-0.2026	-0.1946	328.15	-0.1849	-0.1859
308.15	-0.2022	-0.1929	333.15	-0.1760	-0.1842
313.15	-0.2016	-0.1911	338.15	-0.1682	-0.1824
318.15	-0.1998	-0.1894	343.15	-0.1684	-0.1807
		$w_1 = 0.24$, $w_2 = 0.06$, $x_1 = 0.091$, $x_2 = 0.013$			
298.15	-0.2885	-0.2642	323.15	-0.2787	-0.2453
303.15	-0.2861	-0.2597	328.15	-0.2798	-0.2418
308.15	-0.2845	-0.2560	333.15	-0.2814	-0.2386
313.15	-0.2817	-0.2521	338.15	-0.2843	-0.2365
318.15	-0.2841	-0.2482	343.15	-0.2848	-0.2337
		$w_1 = 0.18$, $w_2 = 0.12$, $x_1 = 0.069$, $x_2 = 0.027$			
298.15	-0.3734	-0.3399	323.15	-0.36096	-0.3109
303.15	-0.3693	-0.3327	328.15	-0.35939	-0.3058
308.15	-0.3660	-0.3270	333.15	-0.35763	-0.3012
313.15	-0.3601	-0.3210	338.15	-0.35708	-0.2986
318.15	-0.3625	-0.3150	343.15	-0.35828	-0.2948
		$w_1 = 0.12$, $w_2 = 0.18$, $x_1 = 0.046$, $x_2 = 0.041$			
298.15	-0.4620	-0.4301	323.15	-0.4350	-0.3919

303.15	-0.4560	-0.4204	328.15	-0.3961	-0.3853
308.15	-0.4488	-0.4129	333.15	-0.4208	-0.3793
313.15	-0.4365	-0.4049	338.15	-0.4317	-0.3763
318.15	-0.4459	-0.3971	343.15	-0.4288	-0.3715
		$w_1 = 0.06$, $w_2 = 0.24$, $x_1 = 0.023$, $x_2 = 0.055$			
298.15	-0.5427	-0.5217	323.15	-0.5137	-0.4737
303.15	-0.5279	-0.5094	328.15	-0.5090	-0.4654
308.15	-0.5342	-0.4999	333.15	-0.5044	-0.4580
313.15	-0.5075	-0.4899	338.15	-0.4984	-0.4543
318.15	-0.5200	-0.4801	343.15	-0.4414	-0.4484
		$w_1 = 0$, $w_2 = 0.30$, $x_1 = 0$, $x_2 = 0.070$			
298.15	-0.6272	-0.6210	323.15	-0.5825	-0.5635
303.15	-0.6166	-0.6062	328.15	-0.5752	-0.5534
308.15	-0.6071	-0.5948	333.15	-0.5689	-0.5447
313.15	-0.5981	-0.5829	338.15	-0.5625	-0.5401
318.15	-0.5900	-0.5712	343.15	-0.5566	-0.5330
		$w_1 = 0.50$, $w_2 = 0$, $x_1 = 0.228$, $x_2 = 0$			
298.15	-0.4456	-0.4400	323.15	-0.4271	-0.4250
303.15	-0.4397	-0.4370	328.15	-0.4257	-0.4220
308.15	-0.4353	-0.4340	333.15	-0.4246	-0.4190
313.15	-0.4314	-0.4310	338.15	-0.4241	-0.4160
318.15	-0.4289	-0.4280	343.15	-0.4239	-0.4130
		$w_1 = 0.45$, $w_2 = 0.05$, $x_1 = 0.207$, $x_2 = 0.014$			
298.15	-0.5843	-0.4468	323.15	-0.4273	-0.4273
303.15	-0.5773	-0.4426	328.15	-0.4236	-0.4235
308.15	-0.5720	-0.4387	333.15	-0.4199	-0.4198
313.15	-0.5659	-0.4347	338.15	-0.4165	-0.4164
318.15	-0.5667	-0.4308	343.15	-0.4130	-0.4129
		$w_1 = 0.40$, $w_2 = 0.10$, $x_1 = 0.186$, $x_2 = 0.028$			
298.15	-0.6071	-0.5400	323.15	-0.5059	-0.5060
303.15	-0.5977	-0.5320	328.15	-0.4997	-0.4998
308.15	-0.5902	-0.5252	333.15	-0.4939	-0.4940
313.15	-0.5838	-0.5182	338.15	-0.4898	-0.4899
318.15	-0.5779	-0.5113	343.15	-0.4847	-0.4848
		$w_1 = 0.30$, $w_2 = 0.20$, $x_1 = 0.142$, $x_2 = 0.056$			
298.15	-0.7759	-0.6489	323.15	-0.7286	-0.5975
303.15	-0.7608	-0.6363	328.15	-0.7212	-0.5882
308.15	-0.7559	-0.6261	333.15	-0.7140	-0.5799
313.15	-0.7447	-0.6155	338.15	-0.7073	-0.5744
318.15	-0.7374	-0.6050	343.15	-0.7040	-0.5673
		$w_1 = 0.20$, $w_2 = 0.30$, $x_1 = 0.097$, $x_2 = 0.086$			
298.15	-0.9541	-0.7937	323.15	-0.8902	-0.7274
303.15	-0.9367	-0.7771	328.15	-0.8809	-0.7155

308.15	-0.9180	-0.7640	333.15	-0.8722	-0.7051
313.15	-0.9118	-0.7504	338.15	-0.8638	-0.6983
318.15	-0.9004	-0.7370	343.15	-0.8570	-0.6893
		$w_1 = 0.10$, $w_2 = 0.40$, $x_1 = 0.049$, $x_2 = 0.116$			
298.15	-1.0701	-0.9422	323.15	-0.9794	-0.8607
303.15	-1.0519	-0.9215	328.15	-0.9790	-0.8462
308.15	-1.0248	-0.9055	333.15	-0.9632	-0.8335
313.15	-1.0135	-0.8888	338.15	-0.9402	-0.8248
318.15	-1.0003	-0.8726	343.15	-0.9211	-0.8138
		$w_1 = 0.05$, $w_2 = 0.45$, $x_1 = 0.025$, $x_2 = 0.132$			
298.15	-1.1180	-1.0192	323.15	-1.0160	-0.9299
303.15	-1.0898	-0.9965	328.15	-0.9965	-0.9139
308.15	-1.0702	-0.9790	333.15	-0.9926	-0.9001
313.15	-1.0529	-0.9607	338.15	-0.9649	-0.8902
318.15	-1.0249	-0.9431	343.15	-0.9048	-0.8780
		$w_1 = 0$, $w_2 = 0.50$, $x_1 = 0$, $x_2 = 0.149$			
298.15	-1.1848	-1.1072	323.15	-1.0847	-1.0101
303.15	-1.1616	-1.0824	328.15	-1.0686	-0.9927
308.15	-1.1400	-1.0635	333.15	-1.0531	-0.9777
313.15	-1.1206	-1.0436	338.15	-1.0381	-0.9666
318.15	-1.1016	-1.0246	343.15	-1.0241	-0.9531

Experimental And Jacob Fitner-Predicted Excess Molar Volumes V_m^E of MEA(1) + 3DMA1P(2) + H_2O(3) Ternary Systems at Different Temperatures (T), Mass (w), Mole (x) fractions and Atmospheric Pressure.

T	**$V_m^E \cdot 10^{-6}$**	**Model**	**T**	**$V_m^E \cdot 10^{-6}$**	**Model**
K	**$m^3 \cdot mol^{-1}$**	**$m^3 \cdot mol^{-1}$**	**K**	**$m^3 \cdot mol^{-1}$**	**$m^3 \cdot mol^{-1}$**
		$w_1 = 0.30$, $w_2 = 0$, $x_1 = 0.113$, $x_2 = 0$			
298.15	-0.2043	-0.1964	323.15	-0.1947	-0.1877
303.15	-0.2026	-0.1946	328.15	-0.1849	-0.1859
308.15	-0.2022	-0.1929	333.15	-0.1760	-0.1842
313.15	-0.2016	-0.1911	338.15	-0.1682	-0.1824
318.15	-0.1998	-0.1894	343.15	-0.1684	-0.1807
		$w_1 = 0.24$, $w_2 = 0.06$, $x_1 = 0.091$, $x_2 = 0.013$			
298.15	-0.2885	-0.2656	323.15	-0.2787	-0.2476
303.15	-0.2861	-0.2613	328.15	-0.2798	-0.2443
308.15	-0.2845	-0.2578	333.15	-0.2814	-0.2412
313.15	-0.2817	-0.2541	338.15	-0.2843	-0.2390

318.15	-0.2841	-0.2505	343.15	-0.2848	-0.2363
		$w_1 = 0.18$, $w_2 = 0.12$, $x_1 = 0.069$, $x_2 = 0.027$			
298.15	-0.3734	-0.3428	323.15	-0.3610	-0.3154
303.15	-0.3693	-0.3361	328.15	-0.3594	-0.3105
308.15	-0.3660	-0.3306	333.15	-0.3576	-0.3061
313.15	-0.3601	-0.3250	338.15	-0.3571	-0.3033
318.15	-0.3625	-0.3194	343.15	-0.3583	-0.2996
		$w_1 = 0.12$, $w_2 = 0.18$, $x_1 = 0.046$, $x_2 = 0.041$			
298.15	-0.4620	-0.4057	323.15	-0.4350	-0.3697
303.15	-0.4560	-0.3965	328.15	-0.3961	-0.3633
308.15	-0.4488	-0.3894	333.15	-0.4208	-0.3578
313.15	-0.4365	-0.3819	338.15	-0.4317	-0.3547
318.15	-0.4459	-0.3746	343.15	-0.4288	-0.3501
		$w_1 = 0.06$, $w_2 = 0.24$, $x_1 = 0.023$, $x_2 = 0.055$			
298.15	-0.5427	-0.5199	323.15	-0.5137	-0.4727
303.15	-0.5279	-0.5078	328.15	-0.5090	-0.4644
308.15	-0.5342	-0.4985	333.15	-0.5044	-0.4572
313.15	-0.5075	-0.4887	338.15	-0.4984	-0.4533
318.15	-0.5200	-0.4791	343.15	-0.4414	-0.4474
		$w_1 = 0$, $w_2 = 0.30$, $x_1 = 0$, $x_2 = 0.070$			
298.15	-0.6272	-0.6210	323.15	-0.5825	-0.5635
303.15	-0.6166	-0.6062	328.15	-0.5752	-0.5534
308.15	-0.6071	-0.5948	333.15	-0.5689	-0.5447
313.15	-0.5981	-0.5829	338.15	-0.5625	-0.5401
318.15	-0.5900	-0.5712	343.15	-0.5566	-0.5330
		$w_1 = 0.50$, $w_2 = 0$, $x_1 = 0.228$, $x_2 = 0$			
298.15	-0.4456	-0.4400	323.15	-0.4271	-0.4250
303.15	-0.4397	-0.4370	328.15	-0.4257	-0.4220
308.15	-0.4353	-0.4340	333.15	-0.4246	-0.4190
313.15	-0.4314	-0.4310	338.15	-0.4241	-0.4160
318.15	-0.4289	-0.4280	343.15	-0.4239	-0.4130
		$w_1 = 0.45$, $w_2 = 0.05$, $x_1 = 0.207$, $x_2 = 0.014$			
298.15	-0.5843	-0.3998	323.15	-0.4273	-0.3849
303.15	-0.5773	-0.3968	328.15	-0.4236	-0.3819
308.15	-0.5720	-0.3938	333.15	-0.4199	-0.3789
313.15	-0.5659	-0.3908	338.15	-0.4165	-0.3760
318.15	-0.5667	-0.3878	343.15	-0.4130	-0.3731
		$w_1 = 0.40$, $w_2 = 0.10$, $x_1 = 0.186$, $x_2 = 0.028$			
298.15	-0.6071	-0.5377	323.15	-0.5059	-0.5073
303.15	-0.5977	-0.5307	328.15	-0.4997	-0.5016
308.15	-0.5902	-0.5247	333.15	-0.4939	-0.4963
313.15	-0.5838	-0.5185	338.15	-0.4898	-0.4920
318.15	-0.5779	-0.5124	343.15	-0.4847	-0.4871

		$w_1 = 0.30$, $w_2 = 0.20$, $x_1 = 0.142$, $x_2 = 0.056$			
298.15	-0.7759	-0.6528	323.15	-0.7286	-0.6068
303.15	-0.7608	-0.6416	328.15	-0.7212	-0.5984
308.15	-0.7559	-0.6326	333.15	-0.7140	-0.5908
313.15	-0.7447	-0.6232	338.15	-0.7073	-0.5850
318.15	-0.7374	-0.6140	343.15	-0.7040	-0.5782
		$w_1 = 0.20$, $w_2 = 0.30$, $x_1 = 0.097$, $x_2 = 0.086$			
298.15	-0.9541	-0.7846	323.15	-0.8902	-0.7226
303.15	-0.9367	-0.7692	328.15	-0.8809	-0.7114
308.15	-0.9180	-0.7570	333.15	-0.8722	-0.7015
313.15	-0.9118	-0.7443	338.15	-0.8638	-0.6941
318.15	-0.9004	-0.7320	343.15	-0.8570	-0.6853
		$w_1 = 0.10$, $w_2 = 0.40$, $x_1 = 0.049$, $x_2 = 0.116$			
298.15	-1.0701	-0.9346	323.15	-0.9794	-0.8556
303.15	-1.0519	-0.9147	328.15	-0.9790	-0.8415
308.15	-1.0248	-0.8992	333.15	-0.9632	-0.8291
313.15	-1.0135	-0.8830	338.15	-0.9402	-0.8200
318.15	-1.0003	-0.8675	343.15	-0.9211	-0.8090
		$w_1 = 0.05$, $w_2 = 0.45$, $x_1 = 0.025$, $x_2 = 0.132$			
298.15	-1.1180	-1.0177	323.15	-1.0160	-0.9298
303.15	-1.0898	-0.9954	328.15	-0.9965	-0.9141
308.15	-1.0702	-0.9782	333.15	-0.9926	-0.9004
313.15	-1.0529	-0.9602	338.15	-0.9649	-0.8904
318.15	-1.0249	-0.9430	343.15	-0.9048	-0.8782
		$w_1 = 0$, $w_2 = 0.50$, $x_1 = 0$, $x_2 = 0.149$			
298.15	-1.1848	-1.1072	323.15	-1.0847	-1.0101
303.15	-1.1616	-1.0824	328.15	-1.0686	-0.9927
308.15	-1.1400	-1.0635	333.15	-1.0531	-0.9777
313.15	-1.1206	-1.0436	338.15	-1.0381	-0.9666
318.15	-1.1016	-1.0246	343.15	-1.0241	-0.9531

Appendix E:

Densities of MDEA + PZ +H_2O ternary solution

30/70 of MDEA/H_2O Experimental Densities ρ of MDEA(1) + PZ(2) + H_2O(3) Ternary Systems at Different Temperatures (T), Mass (w), Mole (x) fractions and Atmospheric Pressure.

T	ρ	T	ρ	T	ρ
K	kg ·m^{-3}	K	kg·m^{-3}	K	kg ·m^{-3}
		$w_1 = 0.301$, $w_2 = 0$, $x_1 = 0.0611$, $x_2 = 0$			
293.15	1025.84	318.15	1013.63	343.15	998.23
298.15	1023.67	323.15	1010.8	348.15	994.83
303.15	1021.37	328.15	1007.84	353.15	991.3
308.15	1018.92	333.15	1004.76	358.15	987.65
313.15	1016.34	338.15	1001.56	363.15	983.84
		$w_1 = 0.293$, $w_2 = 0.025$, $x_1 = 0.0604$, $x_2 = 0.0070$			
293.15	1028.14	318.15	1015.36	343.15	999.55
298.15	1025.84	323.15	1012.43	348.15	996.12
303.15	1023.41	328.15	1009.31	353.15	992.54
308.15	1020.85	333.15	1006.24	358.15	988.74
313.15	1018.17	338.15	1002.97	363.15	984.18
		$w_1 = 0.286$, $w_2 = 0.048$, $x_1 = 0.0602$, $x_2 = 0.0139$			
293.15	1029.43	318.15	1016.32	343.15	1000.27
298.15	1027.08	323.15	1013.33	348.15	996.78
303.15	1024.58	328.15	1010.23	353.15	993.13
308.15	1021.94	333.15	1007.02	358.15	989.4
313.15	1019.19	338.15	1003.7	363.15	985.57
		$w_1 = 0.279$, $w_2 = 0.0698$, $x_1 = 0.0596$, $x_2 = 0.0206$			
293.15	1030.32	318.15	1016.87	343.15	1000.58
298.15	1027.9	323.15	1013.83	348.15	997.01
303.15	1025.32	328.15	1010.68	353.15	993.26
308.15	1022.62	333.15	1007.42	358.15	989.57
313.15	1019.81	338.15	1004.05	363.15	985.73
		$w_1 = 0.272$, $w_2 = 0.091$, $x_1 = 0.0591$, $x_2 = 0.0274$			
293.15	1031.59	318.15	1017.75	343.15	1001.18
298.15	1029.08	323.15	1014.63	348.15	997.58
303.15	1026.41	328.15	1011.44	353.15	993.85
308.15	1023.63	333.15	1008.11	358.15	990.04
313.15	1020.75	338.15	1004.7	363.15	986.15

40/60 of MDEA/H_2O Experimental Densities ρ of MDEA(1) + PZ(2) + H_2O(3) Ternary Systems at Different Temperatures (T), Mass (w), Mole (x) fractions and Atmospheric Pressure.

T	ρ	T	ρ	T	ρ
K	kg ·m^{-3}	K	kg·m^{-3}	K	kg ·m^{-3}
		$w_1 = 0.4000$, $w_2 = 0$, $x_1 = 0.0915$, $x_2 = 0$			
293.15	1036.76	318.15	1022.42	343.15	1005.51
298.15	1034.09	323.15	1019.24	348.15	1001.84
303.15	1031.32	328.15	1015.95	353.15	998.08
308.15	1028.46	333.15	1012.57	358.15	994.22
313.15	1025.5	338.15	1009.11	363.15	990.2
		$w_1 = 0.3902$, $w_2 = 0.0248$, $x_1 = 0.0909$, $x_2 = 0.0080$			
293.15	1037.83	318.15	1023.14	343.15	1005.98
298.15	1035.09	323.15	1019.91	348.15	1002.26
303.15	1032.25	328.15	1016.57	353.15	998.45
308.15	1029.32	333.15	1013.14	358.15	994.58
313.15	1026.28	338.15	1009.61	363.15	990.58
		$w_1 = 0.3813$, $w_2 = 0.0476$, $x_1 = 0.0903$, $x_2 = 0.0156$			
293.15	1038.61	318.15	1023.64	343.15	1006.24
298.15	1035.84	323.15	1020.34	348.15	1002.52
303.15	1032.93	328.15	1016.96	353.15	998.66
308.15	1029.93	333.15	1013.48	358.15	994.73
313.15	1026.83	338.15	1009.91	363.15	990.7
		$w_1 = 0.3721$, $w_2 = 0.0699$, $x_1 = 0.0895$, $x_2 = 0.0232$			
293.15	1039.57	318.15	1024.26	343.15	1006.62
298.15	1036.72	323.15	1020.91	348.15	1002.82
303.15	1033.73	328.15	1017.48	353.15	998.95
308.15	1030.67	333.15	1013.95	358.15	994.98
313.15	1027.51	338.15	1010.32	363.15	990.93
		$w_1 = 0.3640$, $w_2 = 0.0911$, $x_1 = 0.0889$, $x_2 = 0.0308$			
293.15	1040.52	318.15	1024.87	343.15	1006.95
298.15	1037.58	323.15	1021.46	348.15	1003.09
303.15	1034.54	328.15	1017.97	353.15	999.21
308.15	1031.4	333.15	1014.39	358.15	995.2
313.15	1028.18	338.15	1010.72	363.15	991.12

50/50 of MDEA/H_2O Experimental Densities ρ of MDEA(1) + PZ(2) + H_2O(3) Ternary Systems at Different Temperatures (T), Mass (w), Mole (x) fractions and Atmospheric Pressure.

T	ρ	T	ρ	T	ρ
K	kg ·m^{-3}	K	kg·m^{-3}	K	kg ·m^{-3}
		$w_1 = 0.5000$, $w_2 = 0$, $x_1 = 0.1313$, $x_2 = 0$			
293.15	1045.5	318.15	1029.37	343.15	1011.16
298.15	1042.39	323.15	1025.89	348.15	1007.24
303.15	1039.18	328.15	1022.31	353.15	1003.33
308.15	1035.29	333.15	1018.56	358.15	999.26
313.15	1032.55	338.15	1014.99	363.15	995.13
		$w_1 = 0.4882$, $w_2 = 0.0244$, $x_1 = 0.1303$, $x_2 = 0.0090$			
293.15	1046.2	318.15	1029.8	343.15	1011.37
298.15	1043.1	323.15	1026.28	348.15	1007.44
303.15	1039.9	328.15	1022.67	353.15	1003.42
308.15	1036.61	333.15	1018.98	358.15	999.34
313.15	1033.25	338.15	1015.22	363.15	995.17
		$w_1 = 0.4762$, $w_2 = 0.0483$, $x_1 = 0.1291$, $x_2 = 0.0181$			
293.15	1046.74	318.15	1030.08	343.15	1011.44
298.15	1043.58	323.15	1026.5	348.15	1007.48
303.15	1040.32	328.15	1022.86	353.15	1003.45
308.15	1036.97	333.15	1019.12	358.15	999.36
313.15	1033.56	338.15	1015.32	363.15	995.2
		$w_1 = 0.4646$, $w_2 = 0.0700$, $x_1 = 0.1277$, $x_2 = 0.0266$			
293.15	1047.4	318.15	1030.44	343.15	1011.59
298.15	1044.15	323.15	1026.82	348.15	1007.6
303.15	1040.83	328.15	1023.13	353.15	1003.52
308.15	1037.44	333.15	1019.37	358.15	999.38
313.15	1033.98	338.15	1015.52	363.15	995.23
		$w_1 = 0.4549$, $w_2 = 0.0907$, $x_1 = 0.1268$, $x_2 = 0.0350$			
293.15	1047.69	318.15	1030.58	343.15	1011.61
298.15	1044.45	323.15	1027.02	348.15	1007.63
303.15	1041.09	328.15	1023.27	353.15	1003.58
308.15	1037.66	333.15	1019.46	358.15	999.41
313.15	1034.18	338.15	1015.57	363.15	995.25